

**THE INSTITUTE OF PAPER CHEMISTRY, APPLETON, WISCONSIN**

**IPC TECHNICAL PAPER SERIES  
NUMBER 260**

**FURTHER  $^{13}\text{C}$  NMR EVIDENCE FOR THE COEXISTENCE OF  
TWO CRYSTALLINE FORMS IN NATIVE CELLULOSE**

**D. L. VANDERHART AND R. H. ATALLA**

**SEPTEMBER, 1987**

Further  $^{13}\text{C}$  NMR Evidence for the Coexistence of Two  
Crystalline Forms in Native Cellulose

D. L. VanderHart and R. H. Atalla

This manuscript is based on the results of collaboration between The Institute of Paper Chemistry and the National Bureau of Standards, and has been submitted for inclusion in the Symposium on Solid State Characterization of Cellulose, R. H. Atalla, Editor, to be published in the ACS Symposium Series

Copyright, 1987, by The Institute of Paper Chemistry

For Members Only

NOTICE & DISCLAIMER

The Institute of Paper Chemistry (IPC) has provided a high standard of professional service and has exerted its best efforts within the time and funds available for this project. The information and conclusions are advisory and are intended only for the internal use by any company who may receive this report. Each company must decide for itself the best approach to solving any problems it may have and how, or whether, this reported information should be considered in its approach.

IPC does not recommend particular products, procedures, materials, or services. These are included only in the interest of completeness within a laboratory context and budgetary constraint. Actual products, procedures, materials, and services used may differ and are peculiar to the operations of each company.

In no event shall IPC or its employees and agents have any obligation or liability for damages, including, but not limited to, consequential damages, arising out of or in connection with any company's use of, or inability to use, the reported information. IPC provides no warranty or guaranty of results.

Further  $^{13}\text{C}$  NMR Evidence for the Coexistence  
of Two Crystalline Forms in Native Celluloses

D. L. VanderHart

National Bureau of Standards  
Polymers Division  
Gaithersburg, MD 20899

and

R. H. Atalla

The Institute of Paper Chemistry  
Division of Chemical Sciences  
Appleton, WI 54911

The hypothesis that all native celluloses are composites of two crystalline allomorphs,  $I_\alpha$  and  $I_\beta$ , is further explored using solid state  $^{13}\text{C}$  NMR techniques. Spectra of several algal and higher plant celluloses and the effects of acid hydrolysis and mechanical beating are investigated. No significant alteration of the  $I_\alpha$  and  $I_\beta$  ratios is seen upon hydrolysis of a cellulose from cotton linters. However, both beating and hydrolysis enhance the  $I_\beta$  proportion in an algal cellulose obtained from Cladophora. Methods of enhancing the crystalline core resonances, based on proton rotating frame relaxation and carbon longitudinal relaxation, are used to verify that unit cell inequivalence rather than crystal surface chains determines the crystalline resonance profiles. These studies indicate that the C4 resonance region, from 88-92 ppm in all native celluloses is a faithful monitor of the relative numbers of inequivalent sites within the cell(s). Also, the higher plant celluloses contain a much smaller fraction of the  $I_\alpha$  crystalline form than originally proposed. The possibility even exists that the higher plant celluloses represent the pure  $I_\beta$  form. If this is true, then it follows from the C4 lineshape that this unit cell contains more than four non-equivalent anhydroglucose residues.

Experiments based on weak  $^{13}\text{C}$ - $^{13}\text{C}$  spin exchange were also conducted in order to probe the spatial environment, within a 0.7-1.0nm radius, around carbons identified with individual multiplet components, which are assumed to belong exclusively to the  $I_\alpha$  or  $I_\beta$  forms. It is expected that only those carbons belonging to that form will be able

to undergo spin-exchange during a time of 50-70s. The spectrum of such 'nearest neighbors' is isolated for three different multiplet lines in an algal cellulose and two lines in a higher plant cellulose. Results rule out the possibility that tertiary morphology can give rise to any multiplicity in these spectra. Moreover, the results strongly reinforce the hypothesis of polymorphy in the algal celluloses; however, no clear evidence for multiple crystalline forms in the higher plant cellulose is found by this method. The spin-exchange results raise a few minor questions about the details of the spectrum belonging to each allomorph. On the basis of all of these results, revised spectra for the  $I_{\alpha}$  and  $I_{\beta}$  allomorphs are presented. These represent minor departures from the previously published spectra.

Finally, the spectrum of the *Cladophora* cellulose which survived the strong acid hydrolysis closely resembled the cotton hydrocellulose spectrum except that the resolution was much better in the former spectrum. A contrast in resolution is consistent with a difference in the average lateral dimensions for the crystallites; this difference is corroborated by electron microscopy. The close similarity of multiplet relative intensities in these two samples, in spite of their different crystallite surface-to-volume ratios verifies that surface resonances are not determining the apparent multiplet intensities, particularly, for the 88-92 ppm region of the C4 resonance.

## Introduction

In previous publications (1-3) we have proposed, principally on the basis of  $^{13}\text{C}$  NMR evidence, that native celluloses are composites of two crystalline forms occurring in different proportions. These allomorphic forms were designated  $I_{\alpha}$  and  $I_{\beta}$ . The  $^{13}\text{C}$  solid-state spectra proposed for the  $I_{\alpha}$  and  $I_{\beta}$  allomorphs are shown in Figure 1. Although these spectra contain non-crystalline resonance contributions, the crystalline resonance profiles can be distinguished from the non-crystalline resonances due to the greater linewidth and lower total intensity of the latter resonances. The sharp features of the resonance profile are the expression of the two crystalline forms.

The previous studies (1-3) suggested that the higher plant celluloses, like cotton and ramie, were rich in  $I_{\beta}$  while the  $I_{\alpha}$  content was appreciable if not dominant in the algal celluloses and the bacterial cellulose obtained from *Acetobacter xylinum*. In Figure 2 the considerable contrast between the spectra of cotton linter cellulose, both dry (2A) and wet (2B), and algal cellulose (2C) from *Valonia ventricosa* is illustrated. Because the lateral dimensions of the crystallites in cotton are 3.5-5 nm (4-6) and in

Valonia are approximately 12-20nm (7-9), the chains in the former crystallites will have a less defined array of nearest neighbors and be more subject to interfibrillar drying stresses than the Valonia chains. Therefore, the crystalline resonances in spectrum 2A are significantly broader than 2C. Wetting the cellulose relieves drying stresses and sharpens the resonances (10-11) as shown in 2B where the relative multiplet intensities are seen more clearly. The very different multiplet intensities are most obvious at C1 and C4 in spectra 2B and 2C. We postulate that multiple crystalline forms coexist in a given cellulose, arose from the extensive coincidence in the multiplet peak positions and the variation in relative multiplet intensities from cellulose to cellulose. Although other investigators have observed variations of unit cell parameters for the different native celluloses (12-13), differences in numbers of chains per unit cell (14-18), and differences in the -OH stretching regions of IR spectra (19), the possibility that every native cellulose may be polymorphic has only been proposed by us (1-3).

Why an organism should produce more than one kind of crystalline cellulose is not obvious. Moreover, if two crystalline forms coexist, the morphological expressions of each form are not yet recognized, nor have electron diffraction patterns from, say, individual Valonia fibrils yet shown any obvious difference from fibril to fibril (20-21). Therefore, we thought it desirable to examine further the evidence supporting the composite model since the hypothesis has important implications for both biosynthetic and morphological studies.

### Background

At the heart of the interpretation of the  $^{13}\text{C}$  spectra is the postulate that sharper multiplet features associated with chemically equivalent carbon atoms in the cellulose spectra are expressions of magnetically inequivalent sites within the unit cells. If this "fine structure" were due to some other cause, then the conclusion of multiple crystalline forms would be called into serious question. The fact that the ratios of multiplet intensities for given resonances, such as that of C4 or C1, vary from sample to sample and rarely have ratios of small whole numbers, reinforces the crystalline composite hypothesis.

In order to establish further the validity of the hypothesis it is necessary to exclude alternate explanations for the resonance multiplicities. Two possible explanations have been considered in earlier papers and we repeat these here.

The first alternate explanation was that the tertiary structure, i.e. the natural assembly and interweaving pattern of the elementary fibrils may give rise to small shifts and or broadening because of anisotropic bulk magnetic susceptibility (ABMS) (22). This mechanism has been argued previously (23) to give rise to shifts of the order of 0.1 ppm in cellulose; however, this calculation assumed that cellulose possesses an ABMS tensor identical to sucrose. One characteristic of ABMS shifts originating in the tertiary structure is that all carbons within a

given monomer unit should be affected equally by this perturbation. With respect to this measure, the experimental splittings certainly dismiss the dominance of the ABMS mechanism since the lineshapes for, say, C1, C4, and C6 are each different (see Figure 2). However, the possibility that the fine structure is due to a combination of unit cell inequivalence and ABMS effects is more difficult to dismiss and certain results described herein bear directly on this possibility.

The second (and, in our opinion, more likely) alternate explanation is that the surface layers of the crystallites may be well ordered, like those in the crystal interior, and therefore give rise to sharp resonance features which are present in addition to multiplicities arising from inequivalence in those unit cells in the interior of the crystallites. Since the shape and surface-to-volume ratio of native cellulose crystallites vary, the observation that the ratios of multiplet intensities are often not whole numbers could then be explained. In previous reports we have argued (3,23) that surface resonances are not sharp and do not contribute to the multiplicities in the above sense. As evidence against a sharp surface resonance, the intensities of the C4 resonance multiplets in Valonia ventricosa are too large to be explained in this manner. The elementary fibrils of Valonia have typical lateral crystal dimensions of 12x20 nm, so that the outer unit cell layer, assumed for simplicity to be a two-chain unit cell, contains about 20% of the total number of crystal chains. Since the least intense multiplet line represents at least 20% of that carbon's crystalline lineshape intensity, one would have to postulate that both chains in the unit cell on all lateral faces of the crystallite contribute to the same sharp resonance features. This is unlikely. Moreover, in the spectrum of Valonia the broad wings of C4 and C6 are found to comprise about 16-20% of their total intensity and are the most likely manifestations of surface chain resonances. Further evidence regarding this interpretation was sought in the present study.

Our approach to investigating the multiple crystalline form hypothesis in native celluloses is fourfold. First,  $^{13}\text{C}$  spectra of additional native celluloses are examined and further variations are evaluated in the light of the polymorphy hypothesis. Second, variations in the ratio of  $I_{\alpha}$  to  $I_{\beta}$  arising from chemical or mechanical treatments are studied. The crystalline forms may have different sensitivities to chemical attack or mechanical stress so that the  $I_{\alpha}$  to  $I_{\beta}$  ratios could be altered in a given cellulose. This approach requires an independent measurement of any changes in surface-to-volume ratios.

In the third approach, we attempt to isolate or at least enhance those resonances arising from the crystalline interior. If such resonances are enhanced or isolated, then any resonances arising from crystalline surface layers are correspondingly reduced or suppressed.

The fourth and final approach is to probe directly, via  $^{13}\text{C}$  NMR spin exchange techniques, the  $^{13}\text{C}$  resonances lying in the immediate neighborhood, (in this case a sphere of radius 0.7-1.0

nm) of the set of  $^{13}\text{C}$  nuclei giving rise to a particular multiplet component. The idea is that those  $^{13}\text{C}$  nuclei in the immediate neighborhood of, say, a C1 resonance belonging solely to the  $I_{\alpha}$  crystal phase, will also belong principally to the  $I_{\alpha}$  form. However, most of these neighboring  $^{13}\text{C}$  nuclei will not themselves be in the C1 position since  $^{13}\text{C}$  isotopic distributions at natural abundance (1.1%) are quite random. In view of the 0.7-1.0 nm distance involved, several monomer units with their random  $^{13}\text{C}$  site occupation contribute to the C1 neighbors. Thus, if one could isolate the resonance profile of the set of neighbors to the C1 carbons of the  $I_{\alpha}$  form, one would identify all of the carbon resonances associated with the  $I_{\alpha}$  unit cell provided that the unit cell is not too large. Furthermore, the smaller the unit cell, the more faithfully these 'near-neighbor' multiplet intensities would reflect the true multiplet intensities for each carbon in the  $I_{\alpha}$  phase. On the other hand, if ABMS broadening is responsible for producing some multiplet splitting, then the 'near-neighbor' carbon spectrum would show a reduced multiplicity relative to the spectrum of the entire sample.

In this report we present experimental evidence derived from these four approaches. In the end, the hypothesis that unit cell inequivalence alone causes the observed multiplicity for chemically equivalent carbons is supported. Therefore, the crystalline composite hypothesis, although slightly revised, is strongly supported, particularly for the algal celluloses.

### Experimental

$^{13}\text{C}$  spectra were obtained on a spectrometer which operates at a magnetic field of 4.7T (50.3 MHz for carbon).  $^{13}\text{C}$  magnetization was initially generated by spin-lock cross-polarization (24,25) (CP). Magic-angle spinning (26,27) (MAS) speeds were in the range of 3-4 KHz. The rotating rf field strengths for both protons and carbons fell in the range of 60-70 kHz for each nucleus, except for the Dante (28-30) pulses in the  $^{13}\text{C}$  spin exchange experiments. During the Dante pulses rotating rf carbon fields of approximately 10kHz in strength were used in order to suppress CP. CP times of 1 ms were typical. Decoupling periods of 52 ms were employed for signal observation.

Pulse sequences have been described adequately in the literature. In this paper CP or CP-MAS spectra are those obtained via the usual spin-lock CP method (24,25). Spectra relating to the longitudinal relaxation times for carbons ( $T_1^{\text{C}}$ ) were obtained via the method of Torchia (31). In these latter spectra, signals obtained at longer times have enhanced contributions from those carbons with longer  $T_1^{\text{C}}$ 's.

The 'Dante' irradiation is a 'comb' of equally spaced pulses each of which produces a nuclear nutation of only a few degrees (28,29). The object of the sequence is to perturb the Zeeman population of a carbon line at the rf carrier or separated from the rf carrier by the inverse of the time between pulses. In our case a comb of 50 pulses, 1  $\mu\text{s}$  in length and separated by

approximately 0.4 ms, was used to invert (to an extent of about 60% of the original signal amplitude) the multiplet resonance centered on the rf carrier. The inversion of this line is quite efficient, first, because the carbon resonance is well defined due to the presence of proton decoupling during this period and secondly, because the intrinsic  $T_2$  of each frequency is much greater than the apparent  $T_2$  (deduced from linewidth of each multiplet component). A more complete description of the DANTE sequence and its use in selectively perturbing carbon spin populations, even those carbons with sizeable chemical shift anisotropy, may be found in Ref. 30. The Dante sequence is inserted at the beginning of the variable delay time in Torchia's  $T_1^C$  sequence (31).

In this paper, the  $^{13}C$  spin exchange experiments, which employ the Dante sequence, are used to probe the  $^{13}C$  resonance profile of those carbons which lie in an 0.7-1.0 nm sphere surrounding the resonance perturbed by the Dante sequence. A detailed description of the method and a consideration of the spatial extent of  $^{13}C$  spin exchange (or spin diffusion) as a function of time are beyond the scope of this paper. Such information may be found in a forthcoming paper (32). In the present paper the Dante sequence will be viewed as a method for very selectively perturbing the Zeeman spin population within a multiplet.  $^{13}C$  spin exchange in cellulose will be looked upon simply as the mechanism whereby, over the course of the 50-70s mixing period selected for the results shown in this paper, the original spin population disturbance, localized to a given multiplet line in the Dante preparation, spreads to other resonances belonging to carbons within 0.7-1.0 nm of the originally perturbed carbon spins. The method whereby the signals of these neighboring carbons are isolated will be illustrated in the results section. Further details on the validity of this method of separation can also be found elsewhere (32).

All cellulose samples were purified by Browning's method (33) for wood cellulose. Sugar analyses of several of the purified higher plant celluloses revealed a qualitative correlation between the non-glucose pyranoses and the non-crystalline content indicated by the  $^{13}C$  CP-MAS spectra. The algal celluloses and the bacterial cellulose had negligible amounts of non-glucose sugars. With a few noted exceptions, all samples were equilibrated with normal laboratory relative humidity which ranged between 35% and 50%.

Mechanical beating of an algal cellulose from Cladophora glomerata was carried out for 5 hr in a Waring blender at 1% and 3% solids consistency. Beating was judged more efficient in the latter case based on a greater retention of water.

Hydrolysis of the beaten Cladophora was carried out in boiling 4N HCl for 44 hr; mass recovery was 22%. In another preparation, an unbeaten sample from a different strain of Cladophora glomerata, which was harvested from a different location at a different time of year, was subjected to the same hydrolysis conditions; mass yield was 12%. In the latter case, electron microscopic investigation (21) of sonicated and dispersed



fibrils of the original material and of the hydrolyzed material showed no significant change in cross-sectional area. Thus, it appears that the hydrolysis somehow managed to leave the cross sectional area of the remaining fibrils unaffected despite the low mass yield.

The assignment of  $^{13}\text{C}$  resonances to different carbons in the anhydroglucose has been discussed previously (34,35); assignments are also indicated in Figure 1. The broad resonance features upfield from C4 and C6 are due to disorder (3,23,34-36). Non-crystalline resonances associated with the other four carbons more strongly overlap their respective crystalline lines; therefore, the shape of the pure crystalline resonance is most obvious for the C4 and C6 carbons.

## Results

Spectra of Several Native Celluloses. In Figure 3 the CP-MAS spectra of several higher plant celluloses are compared and are also contrasted to the spectrum of algal cellulose from Cladophora glomerata (bottom spectrum). In Figure 4, the spectra of two samples of bacterial cellulose from two different sources of Acetobacter xylinum, several algal celluloses, and the Cladophora, beaten at 1% solids consistency, are shown.

The spectra of the higher plant celluloses in Figure 3 lack resolution in comparison with the algal cellulose spectrum. This poor resolution is most likely attributed to the relatively small lateral dimensions of the crystalline fibrils in these materials. This lack of resolution is generally correlated with the intensity of the broad wings in the C4 and C6 regions. These wings indicate the amount of non-crystalline and/or crystal-surface residues. In Figure 3, the cactus spines and the Benares hemp exhibit the greatest crystallinity, and, to the extent that the downfield portion of the resonance at C4 can be recognized as consisting of three overlapping peaks, the relative heights of the shoulders seem similar to those for cotton (see Figure 2A) suggesting similar  $I_{\alpha}$  to  $I_{\beta}$  ratios. The appearance of a single maximum in certain spectra at C1, for example that of Kenaf, is more an indication of a larger non-crystalline contribution than a greater proportion of the  $I_{\alpha}$  form. This is reasonable since the central maximum is rather broad. The lack of resolution makes measurements of the apparent ratios of  $I_{\alpha}$  to  $I_{\beta}$  difficult.

The lower four spectra in Figure 4 represent four different algal species; Cladophora glomerata, Valonia macrophysa, Rhizoclonium hieroglyphicum, and Valonia ventricosa. These spectra are all quite similar although Cladophora seems to have a slightly larger portion of  $I_{\alpha}$  as judged by the larger downfield shoulder at C4 compared with the upfield shoulder (see Figure 1). The spectrum of Acetobacter at the top of the figure strongly resembles that of Cladophora cellulose. The Acetobacter cellulose contains a larger proportion of non-crystalline material in addition to having a slightly higher proportion of the  $I_{\alpha}$  form according to the spectra of Figure 1. The greater proportion of non-crystalline chains in Acetobacter cellulose is consistent with

a greater surface to volume ratio for the latter since Acetobacter fibrils are approximately 6 nm wide (37) whereas Cladophora fibrils are about 20 nm wide (21). The Valonia, Cladophora, and Rhizoclonium algal spectra each exhibit non-crystalline resonance intensity in the C4 region of the order of 12-20% of the total C4 intensity. The wings of the C4 and C6 resonances in spectrum 4A are more prominent and the crystalline carbon resonances are a bit sharper than in spectrum 4B because the sample in 4A had a higher level of hydration than in 4B.

The spectra of Figure 4 are quite similar, although variations in the heights of the central C1 peaks and the upfield and downfield shoulders of the C4 resonance are outside of experimental error. If the multiplet intensities arise from unit cell inequivalence alone, then these variations support the hypothesis of multiple crystalline forms in the algal and bacterial celluloses.

Spectral Changes Resulting from Mechanical Beating and/or Acid Hydrolysis. The premise underlying this second group of explorations is that two crystalline forms may differ in their response to mechanical or chemical stresses. Thus, one might hope to alter the  $I_{\alpha}$  to  $I_{\beta}$  ratio in a given material after exposure to such stress. On the other hand, the demonstration of such changes would not, in itself, constitute a proof for polymorphy if the multiplet structure in the NMR spectra had its origin, at least partially, in the tertiary morphology or the crystallite surface layers. A complete argument would require that the effect of the applied stresses on these characteristics also be followed.

Figure 5 shows the spectral changes accompanying acid hydrolysis of cotton linters. The hydrocellulose which results from this 30-minute hydrolysis in 2.5N HCl at 100C achieves the leveling-off DP and represents a mass fraction at least 90% of the original (38). Judging by the constant shape of the C4 crystalline resonance (88-92 ppm), no change in the  $I_{\alpha}$  to  $I_{\beta}$  ratio has occurred as a result of hydrolysis. The bottom linear-combination spectrum gives proof that, within experimental error, the C4 (and C6) crystalline resonances are unchanged by the hydrolysis. This linear combination spectrum is very similar to a spectrum of ball-milled, decrystallized cellulose (3) implying that hydrolysis has mainly attacked the 3-dimensionally disordered regions. Since the C4 crystalline resonance is unchanged upon hydrolysis, the corresponding reduction in intensity of the central feature of C1 reflects a decrease in the underlying non-crystalline resonance rather than a change in the  $I_{\alpha}$  to  $I_{\beta}$  ratio.

Figure 6 shows spectra of five preparations of algal celluloses obtained from Cladophora: spectrum A is from the original purified cellulose, spectrum B is that of the same cellulose beaten in a Waring Blender for 5 h while dispersed in water at 1% solids consistency, spectrum C is like B except that the beating was carried out at 3% solids consistency, spectrum D is that of the beaten cellulose in spectrum B following acid hydrolysis in 4N HCl for 44 h at 100 C (22% mass recovery), and

spectrum E is that of the second strain of Cladophora cellulose after purification and exposure only to the above acid hydrolysis (12% mass recovery). The spectrum of the purified cellulose of this second strain is not shown because it is not significantly different from spectrum 6A. Judging by both measures of the  $I_{\alpha}$  content, i.e. the downfield shoulder of C4 (at 90.3 ppm) and the central multiplet feature of C1 (at 105.5 ppm), the  $I_{\alpha}$  content decreased noticeably as a result of beating at both 1% and 3% solids consistency. The degradation of resolution in Figure 6C probably results from a greater alteration of the tertiary morphology in the sample beaten at 3% solids consistency compared with the sample beaten at 1% solids consistency since the former sample retained more water. The strain on the fibrils resulting from the drying of a disordered network would be expected to cause line broadening. Spectrum 6B suggests that some conversion of  $I_{\alpha}$  to  $I_{\beta}$  can be accomplished by mechanical stress since the non-crystalline spectral intensities are very similar in spectra 6A and 6B. However, mass recovery following beating was difficult to monitor. Therefore, while conversion of the  $I_{\alpha}$  to the  $I_{\beta}$  crystalline form via mechanical stress is strongly suggested, the alternate possibility of a preferential mass loss of the  $I_{\alpha}$  form cannot be entirely dismissed.

Scanning transmission electron micrographs of the materials corresponding to spectra 6A and 6B were also acquired. Even though resolution was insufficient for imaging the lateral dimensions of individual crystallites, these micrographs revealed that beating disrupts the fibrillar network. While the original lateral dimensions of most of the fibrillar aggregates were in the 80-200 nm range, aggregates as small as 30 nm could be seen after beating, although the average lateral fibril dimension was about 100 nm. The disruption of tertiary structural organization was thus clear, yet the question of possible alterations of the lateral dimensions of individual crystallites remained unanswered because of insufficient resolution.

The more dramatic spectral changes in Figure 6 are caused by strong acid hydrolysis, rather than beating. Spectra 6D and 6E appear to be "sharper-featured" (more crystalline) versions of the higher plant cellulose spectra (see Figures 2, 3 and 5). There is a dominant upfield shoulder at C4 compared to the downfield shoulder; the central component of C1 is also greatly reduced. The hydrolysis, however, is harsh and a mass loss of 78-88% raises questions about the corresponding changes in lateral crystallite dimensions. If the resonance multiplicity were due, in part, to surface chains, then changes in the lateral dimensions of the crystallites would affect the multiplet intensities. An electron microscopic investigation (21) of the lateral dimensions of sonicated and dispersed individual crystallites showed no significant difference between the celluloses corresponding to spectra 6A and 6E; the lateral dimensions average 20 nm in both cases. The narrower linewidths in spectrum 6E compared with 5A provide additional qualitative support that the average lateral dimensions of the crystallites in the hydrolyzed Cladophora cellulose are substantially greater than those in cotton linters.

(3.5-5 nm) (4-6) and that the sampling of the crystallites in the electron microscopic investigation is representative of the whole material. Thus, the spectral differences between Figures 6A and 6E cannot arise from changes in the number of chains on the crystal surfaces. It follows that the spectra of Figure 6 strongly reinforce the hypothesis that multiple crystalline forms coexist in Cladophora cellulose. Furthermore, they suggest that the  $I_{\alpha}$  form is more susceptible to hydrolysis than the  $I_{\beta}$  form or the  $I_{\gamma}$  form, for morphological reasons, is more exposed to the acid attack.

Methods for Emphasizing Resonance Intensity from Carbons in the Crystalline Interior. The experiments described in this section explore further the possibility that ordered surface layers on crystallites might give rise to sharp resonances, although strong arguments to the contrary have already been given. If one could suppress those resonances arising from crystallite surfaces, then one could isolate the resonance profile corresponding to the true interior unit cell(s) and directly address the question of crystalline polymorphy.

The key assumption in the following experimental approaches is that a chain at the crystalline surface experiences less well-defined, and, on average, weaker intermolecular potentials than an interior crystalline chain. Hence, the surface chain will have a greater molecular mobility and its spins will undergo relaxation more efficiently.

If one further assumes that each nucleus relaxes independently, then one can enhance resonances arising from the crystalline core by isolating those signals corresponding to the most slowly relaxing spins. Observation of  $^{13}\text{C}$  spins only need not limit the study to relaxation characteristics of carbons since the use of CP for  $^{13}\text{C}$  signal generation also gives signals proportional to proton polarization levels (25). Thus, proton relaxation may also be monitored indirectly.

Two questions must be considered when attempting to isolate the crystalline core  $^{13}\text{C}$  spectrum. First, do both protons and  $^{13}\text{C}$  nuclei relax independently? Second, which relaxation parameter will offer the highest contrast between surface and interior resonances?

Observations based on proton spin diffusion. Protons, by virtue of their 100% natural abundance are strongly coupled to one another by dipolar coupling. This coupling gives rise to spin exchange which, in turn results in spin diffusion (39) whereby magnetization is transported in a diffusion-like process. When protons are quantized along the static field, a diffusion constant of about  $5 \times 10^{-12} \text{ cm}^2/\text{s}$  is appropriate for cellulose (40); in the presence of a strong, resonant proton rf field, the diffusion constant is halved. We find that the longitudinal and rotating frame relaxation times ( $T_1^{\text{H}}$  and  $T_{1\rho}^{\text{H}}$ ) in cellulose are respectively in the ranges of 0.5-6s and 15-120ms. Proton spin diffusion will thus maintain very uniform spin polarization levels during a  $T_1^{\text{H}}$  recovery so that monitoring  $^{13}\text{C}$  spectra as a function

of proton recovery time will not reveal any contrast in intensity between surface and interior chains. On the other hand, times like 15-20ms, which are typical (41) values for  $T_{1\rho}^H$  in higher plant celluloses are comparable to times expected for magnetization transport across a crystallite 3.5-5 nm in lateral dimension (42,43). Therefore, if one obtains CP spectra using a fixed CP time applied at the end of a variable proton spin-locking time, the core crystalline resonances would be enhanced at longer spin-locking times. However, the spectra would never be entirely free of the surface resonances. (A superior experiment and one which we did not do because of its technical difficulty is to monitor the CP spectrum following a period of relaxation under multiple pulse (43,44). The multiple pulse irradiation simultaneously attenuates spin diffusion very strongly.)

Figure 7 shows spectra of hydrocellulose obtained from cotton linters using a CP time of 0.5 ms. For spectrum A the spin locking time prior to CP was 0.01 ms while in spectrum B it was 25 ms. The 'A-B' spectrum shows that the shapes of the C4 crystalline resonances in A and B are indistinguishable in spite of the proton magnetization gradient between the surface and the interior of the crystallites. The existence of this gradient is confirmed by the preferential reduction of the broad resonances in B relative to A. Most of the intensity in these broad resonances in the hydrocellulose, we believe, arises from crystal surface chains, although alternative interpretations have been proposed (36), namely, that all intensity in the wings of C4 and C6 arises from non-crystalline carbons. In support of our point of view, we note the contrast in shape between this difference spectrum in Figure 7 and that of Figure 5C, particularly in the C2,3,5 region. In cotton linters the C2,3,5 carbons in three-dimensionally disordered regions contribute to the single broad resonance; but these regions are attacked preferentially during hydrolysis. In the difference spectrum of Figure 7, the C2,3,5 resonance region has much more definition as one might expect from more ordered surface chains. The other difference spectrum at the bottom of Figure 7 indicates that there is no further lineshape change occurring for spin-locking times longer than 15 ms. Stabilization of the lineshape by proton spin diffusion at about 15 ms is quite consistent with expectations (42) if most of the disordered, more mobile material were on the surface of crystallites whose lateral dimensions were in the 3.5-5 nm range. Thus, under the assumption that the surface chain protons have shorter intrinsic  $T_{1\rho}^H$  values than do the interior chain protons, these results indicate that the shape of the C4 resonance contains no sharper features (in the range from 88-92 ppm) associated with surface chains. Also, since the proton polarization is not expected to vary appreciably over dimensions of monomer units, the resonance profiles for each carbon in the difference spectrum arise from the same spatial regions. Therefore, the monomer units which give rise to the broad C4 resonance also produce a corresponding contribution to the central region of the C1 resonance.

A similar  $T_{1\rho}^H$  experiment was conducted on algal cellulose from Rhizoclonium. Figure 8 shows these results and the difference spectrum. Because the lateral crystallite dimension in Rhizoclonium is 25-30 nm, the contrast, after an extended period of spin-locking, between average proton magnetization at the surface and in the crystallite interior can become larger than in hydrocellulose, even though the apparent  $T_{1\rho}^H$  increases fivefold to about 100 ms. Nevertheless, no change in the C4 lineshape is observed as a function of spin-locking time. Again we conclude that surface resonances are not contributing to the fine structure at C4. In fact, none of the sharp resonances seem to change relative intensity with spin locking times. The implication is that these sharp features are the expression of the true unit cell(s).

Observations based on  $^{13}C$  longitudinal relaxation with spin exchange. Depending on the type of native cellulose, the  $^{13}C$  longitudinal relaxation time,  $T_1^C$ , for each crystalline carbon at 50 MHz can become quite long. In hydrocellulose, for example, crystalline  $T_1^C$ 's are of the order of 200s (45) while in the algal celluloses we find that corresponding  $T_1^C$ 's are closer to 1000s. Thus, the  $T_1^C$ 's in these systems are sufficiently long to allow some  $^{13}C$ - $^{13}C$  spin exchange to occur.

The influence of  $^{13}C$  spin exchange on  $T_1^C$  is non-existent when all carbons have the same intrinsic relaxation time. However, at 50MHz the  $T_1^C$  values for the broad resonance of C6 are less than 1s and the  $T_1^C$  for the broad resonance of C4 is about 10-20s (45). A fraction of faster relaxing intensity, comparable to that at C4, is also visible in the other resonances at C1 and C2,3,5. If one assumes that most of this faster relaxation is occurring at the crystalline surface and in 3-dimensional regions of disorder; then, by  $^{13}C$  spin exchange, crystalline carbons about 1 nm from the surface will also relax more efficiently. Therefore, the most slowly relaxing carbons in a  $T_1^C$  experiment will be those associated with the crystalline core.

Figures 9 and 10 show spectra of cotton hydrocellulose and cellulose from Cladophora, respectively, as a function of delay time in Torchia's  $T_1^C$  method (31). At longer delay times, these spectra represent the  $^{13}C$  nuclei not yet relaxed. The disappearance of the broad features and the slight sharpening of the crystalline resonances are consistent with an enhancement of the crystalline core resonances since the most highly ordered chains should produce the sharpest resonances (22).

Figure 9 raises an important question concerning crystalline polymorphy in the native celluloses. The hypothesis that higher plant celluloses like cotton and ramie are crystalline composites was suggested, in part, by the outer doublet and the sharper central feature of the C1 resonance in spectrum 9A. However, comparison of spectra 9A and 9C shows the central peak at C1 to be less intense at 200s compared with 1 ms, while the shape of the crystalline resonance at C4 remains constant. Since carbons C1-C5 relax at very nearly the same rates (32) in a  $T_1^C$  experiment, it is very likely that the signals for each of these carbons in

spectrum 9C arise from the same spatial regions. Thus, the composite hypothesis would lead one to expect a smaller downfield shoulder at C4 than is observed in Figure 9C. The difference spectrum, A-C, is very similar to the difference spectrum in Figure 7 and shows that the change of shape at C1 does not involve any particularly sharp component; in fact, the corresponding resonance change at C4 involves the broad upfield shoulder. Therefore, the lineshape change at C1 is attributed to anhydroglucose residues in disordered regions, probably including the crystal surface. This leaves less of the central resonance intensity at C1 which can be ascribed to the presence of the  $I_{\alpha}$  phase. If there is an  $I_{\alpha}$  crystalline polymorph present, it is of the order of 15% or less.

Since we believe that spectrum 9C, in all regions except C6, possesses undistorted relative intensities whose dominant contributions arise from chains in the crystalline core, the following alternative interpretation must be considered: (a) The originally postulated (1-3)  $I_{\alpha}$  phase in cotton or ramie is no more than a minor component. (b) Because the downfield shoulder of C4 and the central component of C1 are becoming comparable in intensity, the originally suggested spectrum of the  $I_{\beta}$  form may not be accurate (see Figure 1) since the intensity of the C1 resonance in the  $I_{\alpha}$  phase should be twice that of the downfield shoulder of C4. (c) Because of (b) the possibility exists that Figure 9C is the correct  $I_{\beta}$  lineshape (except in the C6 region). (d) If Figure 9C represents the true  $I_{\beta}$  lineshape, then the multiplet ratios of C4 require that the unit cell must contain more than four anhydroglucose units in order to generate these intensity profiles. (e) The C4 crystalline resonance (88-92 ppm) in spectrum 9A is a good indicator of the number of carbons at each magnetically distinct site in the unit cell.

In contrast to the difference in the behavior of the C1 and C4 lineshapes for cotton hydrocellulose in Figure 9, the changes in lineshape for Cladophora cellulose in Figure 10 are very minor. Since the crystallite width in Cladophora cellulose is about 20 nm (21), the intensity change related to crystal surface resonances is expected to be reduced. Thus, the principal changes between spectra 10A and 10C involve a slight sharpening of the resonances in spectrum 10C and a disappearance of the weak, broad C4 and C6 wings. All the celluloses represented in Figure 4 showed similar  $T_1^C$  behavior. Again, we interpret spectrum 10C as arising principally, from chains in the crystalline interior. In Figure 10 there is no anomalously fast decay associated with the sharp central feature of C1 as there was in Figure 9. The overall decay of intensity for Cladophora cellulose during the 200s was 32% compared with 77% for the hydrocellulose in Figure 9. Much of this difference in extent of decay can be explained by the larger crystallites in Cladophora cellulose, the associated reduction in the number of more mobile surface chains and the diminished opportunity for spin exchange with these surface chains.

Figure 10 indicates that: (a) If two allomorphs coexist in the Cladophora cellulose, the  $T_1^C$  behavior of both allomorphs is the same. (b) If the reduction of intensity in the  $T_1^C$

experiments is principally due to  $^{13}\text{C}$ - $^{13}\text{C}$  spin exchange with surface chains, then the stability of the lineshapes in Figure 10 suggests that the surface-to-volume ratios, or the lateral dimensions of the  $I_\alpha$  and  $I_\beta$  crystallites are comparable. (c) The resonance profiles, especially for C4 (88-92 ppm), in spectrum 10A give a good indication of the relative number of carbons at each of the magnetically inequivalent sites in the unit cell(s).

Isolation of Spectra from Carbons Within 0.7-1.0 nm of a Carbon in a Single Multiplet Line.  $^{13}\text{C}$ - $^{13}\text{C}$  spin exchange is quite slow in a natural abundance sample when proton decoupling is absent. The rate of exchange depends, among other things, on the inverse sixth power of the  $^{13}\text{C}$ - $^{13}\text{C}$  internuclear distance (39,46). At natural abundance, these distances are statistically determined; moreover, the nearest  $^{13}\text{C}$  neighbors to a given carbon, say C1, will generally not be C1 carbons. Because a more complete treatment of this experiment and its interpretation will appear elsewhere (32), we will simply take a descriptive approach.

Isolation of the spectra of neighboring  $^{13}\text{C}$  nuclei is as follows: a) The Zeeman population of one line within a multiplet is perturbed using the Dante (28,29) sequence. b) After the perturbation a 50s-70s mixing time follows during which magnetization changes occur due to both  $T_1^{\text{C}}$  processes and  $^{13}\text{C}$ - $^{13}\text{C}$  spin exchange. c) The spin exchange and the  $T_1^{\text{C}}$  effects are monitored independently to isolate the 'near-neighbor' spectra associated only with those carbons which have undergone spin exchange as a result of the original perturbation.

These 'near-neighbor' spectra arise from carbons primarily lying within a radius of 0.7-1.0 nm from the perturbed carbons. (32). Such 'near-neighbor' spectra are a simultaneous test of the alternate explanations for the observed differences in native cellulose spectra, namely, that some sharp spectral features originate from chains on crystallite surfaces or that ABMS effects give rise to sharp features because of special tertiary morphology. The choice of the perturbed line is based on the  $I_\alpha$  and  $I_\beta$  spectra of Figure 1 such that the perturbed line belongs either to the  $I_\alpha$  or  $I_\beta$  spectrum. For this purpose, the C1 and C4 resonances are best since there is significant overlap elsewhere.

Figure 11 illustrates the application of this technique to a sample of Rhizoclonium cellulose. Spectrum 11A and 11B are different only in that the low-level 'comb' of  $^{13}\text{C}$  Dante pulses is absent (11A) or present (11B). Proton decoupling was applied for 20ms during the Dante sequence; this decoupling was also present in the experiment without the Dante pulses in order to make comparison between these two experiments most meaningful. The 3ms interval indicated in Figure 11 refers to the period between the end of the Dante pulses and the beginning of signal observation. Spectra 11C and 11D are pairs similar to 11A and 11B except that the mixing time was 70s instead of 3ms. Spectra 11E-11G are each difference spectra based on spectra 11A-11D. Spectrum 11E represents the profile of the original population disturbance produced principally at the central C1 multiplet in Rhizoclonium cellulose (an ' $I_\alpha$ ' perturbation - see



Figure 1). Spectrum 11F is the 'near-neighbor' spectrum which also includes a rather large peak corresponding to the C1 sites which have not yet exchanged. Figure 11G is a more amplified (x2) near-neighbor spectrum obtained by subtracting a portion of spectrum 11E from 11F in order to decrease the intensity in the central C1 region and also look for possible 'near-neighbor' lines corresponding to the outer wings of the C1 resonance which are thought to belong to the  $I_{\beta}$  allomorph. In other words, spectrum 11G tests whether the profile of the C1 resonance has changed as a result of  $^{13}\text{C}$ - $^{13}\text{C}$  spin exchange with other C1 multiplets. The lack of wing intensity at C1 argues against the suggestion of Cael, et al. (47) that the central resonance of C1 belongs to a unit cell possessing a 1:2:1 triplet.

Several conclusions may be drawn from Figure 11. First, this Dante sequence is quite selective. Spectrum 11E shows that the population disturbance is centered quite well on the central C1 multiplet. Second, the 'near-neighbor' spectrum may be isolated (Spectrum 11F) and even tested for spin exchange within the C1 multiplet (spectrum 11G). Third, given that the perturbation is thought to be an ' $I_{\alpha}$ ' perturbation (see Figure 1), the 'near-neighbor' spectrum contains many characteristics typical of an  $I_{\alpha}$ -rich spectrum, i.e. weak C1 doublets, a strong downfield shoulder at C4, and a sharp maximum at the correct position for C6. The profile of the C2,3,5 region deviates somewhat from the  $I_{\alpha}$  spectrum of Figure 1; however, this region in Figure 1 has a substantial non-crystalline contribution and a lower intrinsic resolution which makes comparison more difficult. Qualitatively, the departure of the 'near-neighbor' spectrum (11G) from the parent spectrum (11A) supports the idea of crystalline polymorphy. Fourth, from a qualitative point of view,  $^{13}\text{C}$ - $^{13}\text{C}$  spin exchange seems quite uniform in the sense that the 'near-neighbor' spectra have intensities at C4 and C2,3,5 which are in the ratio 1:3 with C6 being slightly less intense (80% of C4 intensity), as expected. Moreover, the total intensity in spectrum 11F was found to be 90% of the total intensity in spectrum 11E which corresponds quite well with expectations based on the 15% decay over 70s of the central C1 multiplet due to  $T_1^C$  processes (spectra 11A and 11C). This agreement ensures that the 'near-neighbor' spectrum is not due to a change in spectrometer characteristics. The ratio of the C1 intensity to the total intensity in spectrum 11F indicates that slightly more than half of the intensity at C1 in spectrum 11E has, over 70s, made its way to other carbon sites via  $^{13}\text{C}$ - $^{13}\text{C}$  spin exchange. Fifth, most of the multiplet lines seen in the parent spectrum (11A) are also seen in the 'near-neighbor' spectrum (11F, 11G). It follows that ABMS effects are probably insignificant (this is shown more rigorously later).

In order to demonstrate crystalline polymorphy more fully, Figure 12 shows the results of three Rhizoclonium cellulose experiments, like those of Figure 11, in which three different lines were initially perturbed. Spectrum 12A is the parent spectrum (like spectrum 11A). The remaining six spectra, in three pairs, consist of profiles of an original population perturbation (like spectrum 11E) caused by the Dante inversion followed by the

corresponding 'near-neighbor' spectrum. The 'near-neighbor' spectra are like those of spectrum 11G except that a null in the position of the perturbed site is not sought; rather, an intensity comparable to the site intensities at the neighboring sites is left at the originally perturbed site, i.e., an 'equilibrium' spectrum is approximated. Spectra 12B and 12C as well as 12D and 12E correspond to ' $I_{\beta}$ ' perturbations (see Figure 1) while spectra 12F and 12G correspond to the ' $I_{\alpha}$ ' perturbation of Figure 11. The Dante sequences used here are not ideal in their ability to select a multiplet line; there is some perturbation of the adjacent line as well. This non-ideality is more apparent when the perturbed line is weaker than the adjacent line as is the case in spectra 12C and 12E. In spite of this non-ideality, the 'near-neighbor' spectra resulting from these ' $I_{\beta}$ ' perturbations are very similar to one another in resonance position and reasonably similar in intensity profiles. These two 'near-neighbor' spectra also show many features which indicate that the  $I_{\beta}$  content (see Figure 1) of each spectrum is much higher than in the parent spectrum (12A) as expected for a mixture of crystalline polymorphs. The strongly emphasized C1 doublet, the dominant upfield shoulder of C4, and the flatter profile for the C6 maximum are all consistent with an  $I_{\beta}$ -rich spectrum. These spectra stand in contrast to the previously discussed  $I_{\alpha}$ -rich spectrum (12G). The upfield portion of the C2,3,5 resonances in the 'near-neighbor' spectra also follows expectations based on the spectra of Figure 1. The non-trivial central component of C1 in spectra 12C and 12E may be no accident since the results of Figure 9, as discussed earlier, may point to an  $I_{\beta}$  spectrum which includes a weak central C1 resonance.

A number of conclusions follow from Figure 12. These are: a) Assuming that the pure  $I_{\alpha}$  and  $I_{\beta}$  spectra are given in Figure 1, an ' $I_{\alpha}$ ' or ' $I_{\beta}$ ' initial perturbation yields a 'near-neighbor' spectrum which is richer, compared with the parent spectrum, in the corresponding ' $I_{\alpha}$ ' or ' $I_{\beta}$ ' resonances. This is illustrated most clearly in the C4 crystalline resonance profiles of the 'near-neighbor' spectra. b) The two 'near-neighbor' spectra resulting from the  $I_{\beta}$  perturbation are very similar to one another indicating that the intensities in the 'near-neighbor' spectra are not very dependent on the line which is perturbed. c) The insignificance of ABMS shifts is indicated by the 'near-neighbor' spectrum, 12C. For if it is postulated that ABMS shifts appear in discrete bands (as opposed to a continuum) as a result of well-defined fibril patterns, and if unit cell multiplicity also exists, then the resonance profile for a given carbon is the convolution of the two effects. Since the origin of the ABMS effects is postulated to be the fibril packing geometry, the dimensions involved are much larger than the unit cell. This implies that all spectral lines associated with unit cell inequivalence are, within any given unit cell, shifted to the same extent as a result of ABMS effects; moreover, if two outer bands exist (e.g. for C1 and C4) each outer band must belong to a different set of ABMS-shifted sites. The fact that the 'near-neighbor' spectrum, 12C, resulting from the perturbation of

one outer C4 band shows spin-exchange with both outer C1 bands is, therefore, a contradiction of the original postulate since spin exchange is too slow to occur between fibrils. So ABMS effects and the importance of fibril geometry are dismissed as a possible cause of any multiplet character for all resonances. d) None of the minor resonances at C1 or C4 are exclusively due to surface chains because the crystallites in *Rhizoclonium* cellulose have lateral dimensions of the order of 25-30 nm; therefore, the total fraction of surface chains is less than 13%, considering both chains in a two chain unit cell at the crystalline surface to be surface chains. No minor resonance at C4 or C1 is as small as 13% in spectrum 12A. Moreover, the 'near-neighbor' spectra (12C and 12E) resulting from the perturbation of minor resonances at C4 and C1 indicate spatial proximity with carbons resonating at several multiplet lines of the unperturbed carbons (C1 or C4). These demonstrated proximities to carbons, if by hypothesis located at a crystal surface, multiplies the number of resonances associated with crystallite surfaces, and also thereby increases unreasonably the total intensity attributable to surface chains. e) The final conclusion based on Figure 12 is that the 'near-neighbor' spectra, while certainly becoming richer in the spectrum of the allomorph to which the perturbed carbon was thought to belong, still retain a significant contribution from the spectrum of the other allomorph. Part of the explanation for this lies in the slight non-ideality of the perturbation. However, judged by the pure  $I_{\alpha}$  and  $I_{\beta}$  spectra of Figure 1, the ratios of  $I_{\alpha}$  and  $I_{\beta}$  in the 'near-neighbor' spectra (Figures 12C, 12E, and 12G) do not agree particularly well with the apparent ratios deduced from the perturbation profiles (Figures 12B, 12D, and 12F). Thus, while crystalline polymorphy is strongly supported by the results, some details of the actual  $I_{\alpha}$  and  $I_{\beta}$  spectra of Figure 1 are called into question. For example, the absence of a central component at C1 in the  $I_{\beta}$  spectrum is questioned. Also the absence of a weak downfield wing at C4 in the  $I_{\beta}$  spectrum and the absence of a weak C4 upfield wing in the  $I_{\alpha}$  spectrum are questioned. Finally, the singlet character of C6 in the  $I_{\alpha}$  spectrum is also questioned (see spectrum 12G). Admittedly, one of the original criteria we applied (1-3) in postulating the  $I_{\alpha}$  and  $I_{\beta}$  spectra of Figure 1 was to minimize the number of magnetically inequivalent sites within the spectrum of each allomorph. In fact the results of both Figures 9 and 12 suggest that the unit cell of each allomorph may contain more than two magnetically inequivalent sites, hence, larger or less symmetric unit cells.

With regard to the question of whether the higher plant celluloses contain only one crystalline allomorph, namely,  $I_{\beta}$ , two  $^{13}\text{C}$  spin exchange experiments were also carried out on hydrocellulose from cotton linters. Figure 13, which is in the same format as Figure 12, shows these results. For reasons of sensitivity, only a 50ms mixing time was used to generate the 'near-neighbor' spectra. This shorter mixing time reduces only slightly the spherical volume around the perturbed carbon probed by spin exchange. The two sites of perturbation are the central

resonance of C4 (spectra 13B and 13C) and the central resonance of C1 (spectra 13D and 13E). The central resonance of C4 is expected (see Figure 1) to belong equally to both the  $I_\alpha$  and  $I_\beta$  allomorphs. Therefore, the corresponding 'near-neighbor' spectrum should give back both the  $I_\beta$  and any  $I_\alpha$  contributions at C1. In spectrum 13C, there is no indication of a central feature at C1 although it is difficult to get sufficiently good signal-to-noise to eliminate a weak central component at C1. On the other hand, the 'near-neighbor' spectrum (13E) from the perturbation of the central C1 region consists of weaker resonances, compared with spectrum 13C; also the resonances seem rather broad and ill-defined. From Figure 9 we know that  $T_1^C$  in the central C1 region is shorter than for other crystalline resonances; therefore, spectrum 13E is weak. However, if there were an  $I_\alpha$  component in the higher plant celluloses, then one might have expected some sharper resonance features associated with the  $I_\alpha$  allomorph in spectrum 13E. Because of the rather poor signal-to-noise, sharper resonance features are difficult to identify. It is significant, however, that the 'near-neighbor' spectrum, 13E, contains some intensity in the regions of the crystalline C4 and C6 carbons. The results of Figure 13 together with those of Figure 9 leave open the distinct possibility that the higher plant celluloses represent a single crystalline allomorph whose crystalline spectrum is very much like that of Figures 9C or 13C. Then it would follow that the number of anhydroglucose units per unit cell is larger than four, (more than two chains per unit cell) judging by the intensities of the multiplet at C4. At the same time the presence of a small  $I_\alpha$  fraction is still possible; however, it is doubtful that there is enough of the  $I_\alpha$  present to account fully for the downfield wing of C4. Therefore, a unit cell with more than four inequivalent anhydroglucose units must be considered likely.

Finally, the question arises as to the true spectrum for each allomorph in native cellulose. Figure 14 shows candidate spectra for the  $I_\alpha$  and  $I_\beta$  allomorphs based on linear combinations of the original and hydrolyzed Cladophora cellulose spectra of Figure 6A and 6E. These spectra are reproduced in spectra 14A and 14B. The latter spectrum strongly resembles the spectrum of the regenerated cellulose I which was originally used (1-3) as the  $I_\beta$ -rich spectrum for generating the  $I_\alpha$  and  $I_\beta$  spectra. The spectrum of the regenerated cellulose I had inferior resolution compared with 14B, so it was not used. Figure 14C is the  $I_\alpha$  spectrum and Figures 14D and 14E are two candidates for the  $I_\beta$  spectrum. Spectrum 14D is based on the original idea (1-3) that the  $I_\beta$  resonance at C1 is a doublet, whereas spectrum 14E considers the  $I_\beta$  spectrum to be that which duplicates the higher plant cellulose C4 and C1 crystalline resonances (see the discussions of Figures 9 and 13 above).

If spectra 14C and 14D are the true spectra of the  $I_{\alpha}$  and  $I_{\beta}$  allomorphs, then, judging by the C4 and C6 resonances, each of the two unit cells contain only two equally-occupied magnetically inequivalent anhydroglucose sites. On the other hand, if spectrum 14E is the true  $I_{\beta}$  spectrum, then the intensity ratio at C4 implies a unit cell with at least three magnetically inequivalent sites in such a ratio as to require a unit cell with more than four anhydroglucose units. To entertain the notion of non-equivalent anhydroglucose units along any given chain (48-50) certainly seems appropriate in this context. The number of resonances in the C1 and C2,3,5 regions generally support the foregoing comments about magnetic inequivalence; these resonances, however, are less informative than the C4 and C6 resonances because the crystalline and the non-crystalline (or surface) carbon resonances at each site overlap strongly. One cannot easily improve the analysis for the C1 and C2,3,5 regions by isolating and subtracting the shape of the resonance which does not belong to the crystal. Evidence points to a variation from sample to sample in the shape of this resonance, presumably because the ratio of surface chains to chains in three-dimensionally disordered environments is sample dependent.

#### Summary

The hypothesis (1-3) that all native celluloses are a composite of two crystalline allomorphs, designated  $I_{\alpha}$  and  $I_{\beta}$ , has been further tested using  $^{13}\text{C}$  solid state NMR. In particular, two alternate origins of sharp resonance features were considered in addition to the usual origin, the crystalline unit cell. The first source is ordered layers on crystal surfaces; the second is possible anisotropic bulk magnetic susceptibility (ABMS) shifts associated with well defined fibril patterns (tertiary morphology).

A survey of several native celluloses reinforced the similarity of the higher plant celluloses to one another, although limits of resolution and questions of chemical purity in the cellulose chains make comparison difficult and less meaningful. A parallel survey of NMR spectra from the more chemically pure algal celluloses and the bacterial cellulose, Acetobacter xylinum, indicated a general uniformity, albeit these spectra were distinct from the spectra of the higher plant celluloses. These algal cellulose spectra, however, showed small variations, outside of experimental error, which were taken as evidence for crystalline polymorphy.

Exposure of cotton linters to acid hydrolysis did not alter the  $I_{\alpha}$  to  $I_{\beta}$  ratios, judging by the C4 resonance profile. On the other hand, exposure of the algal cellulose from Cladophora to mechanical beating and/or strong acid hydrolysis caused changes in the NMR spectra, which, in the crystalline composite model, would be interpreted as enriching the  $I_{\beta}$  content of the spectra. Acid hydrolysis was more effective than beating in changing the apparent  $I_{\alpha}$  to  $I_{\beta}$  ratio. Whether the enrichment of the  $I_{\beta}$  content by beating was accomplished via a differential mass recovery or an actual conversion of one allomorph to the other is not clear. The

acid hydrolysis, on the other hand, was harsh and material recovery was only 12-22%. Therefore, the differences in rates of hydrolysis between the  $I_{\alpha}$  and  $I_{\beta}$  allomorphs may not be large. It is possible that differences in hydrolysis rates are related to morphology and the physical access of the acid to the crystallites rather than a greater inherent resistance to hydrolysis of the  $I_{\beta}$  allomorph. However, an important observation is that sonicated and dispersed individual crystallites from the extensively hydrolyzed cellulose did not show, by electron microscopy, any reduction in cross-sectional area compared to the original cellulose crystallites; therefore, spectral changes resulted from a selection process rather than from an alteration of the surface-to-volume ratio of crystallites. The NMR spectrum of the hydrolyzed algal cellulose strongly resembled the spectra of the higher plant celluloses, except for the much better resolution in the former spectrum. (The improved resolution is very consistent with a much greater lateral crystallite dimension.) The similarity, except for resolution, of the multiplet intensities in spectra of the hydrolyzed Cladophora (Figure 6E) and of the higher plant celluloses (Figure 7B) is strong evidence that ordered layers on crystal surfaces are not responsible for the multiplet intensity patterns, particularly at C4, in the higher plant cellulose spectra. Or, from a different perspective, the similarity of these spectra supports the existence of a crystal structure associated with the higher plant celluloses, i.e., the small crystallite width does not lead to a more statistical assembly of chains.

A set of experiments aimed at enhancing the core crystalline resonances over the crystalline surface chain resonances was also undertaken. The approaches, which utilized  $T_{1\rho}^H$  and  $T_1^C$  relaxation behavior, were predicated on the existence of greater molecular mobility (enhanced relaxation rates) for chains at the crystal surface relative to the crystallite interior. Strong proton-proton spin exchange during  $T_{1\rho}^H$  relaxation blurs somewhat the differences between surface chain and interior chain relaxation; nevertheless, this approach has the advantage that the  $^{13}C$  CP spectra, taken as a function of the  $T_{1\rho}^H$  decay, have undistorted intensities over dimensions of monomer units. On the other hand,  $T_1^C$  relaxation is much more a function of the individual carbons;  $^{13}C$ - $^{13}C$  spin-exchange is weak. Therefore one has an excellent opportunity to see differential effects due to molecular mobility variations. In this case, it is not obvious that spectra should retain undistorted relative intensities. Fortunately, however, and probably due to a combination of weak  $^{13}C$ - $^{13}C$  spin exchange and the relative rigidity of the pyranose ring, the resonance profiles of carbons C1-C5 seem to be undistorted, i.e. on average, the C1-C5 carbons in the same spatial region give identical contributions to the observed intensity during a  $T_1^C$  decay. The important conclusions of these relaxation experiments are the following: If crystal surface chains are more mobile than interior chains so that the nuclei on the former chains relax more efficiently than their interior-chain counterparts, then: a) the C4 crystalline resonance profile is

unchanged (except for a slight sharpening of the multiplet lines) as one enhances the relative resonance contribution from the crystalline core. Therefore, C4 is the best indicator of multiplicity related to the true crystalline unit cell(s), i.e. surface-chain resonances do not make a significant contribution to the multiplet intensities there. b) The higher plant celluloses are seen to possess only a minimal  $I_{\alpha}$  content (15% or less). In fact, the  $I_{\alpha}$  content may be zero. If so, the true unit cell inequivalences, which are best expressed by the multiplet intensities within the C4 resonance profile, lead to a unit cell containing more than four anhydroglucose residues. Even with a 15% contribution from the  $I_{\alpha}$  form, it is doubtful that the intensity of the downfield multiplet component of C4 could be fully accounted for. Therefore, the likelihood that the  $I_{\beta}$  crystalline form, which dominates the higher plant celluloses, has more than four anhydroglucose residues per unit cell is very high. c) The algal celluloses display no discernible change in multiplet relative intensities in a  $T_1\rho$  experiment, thus it is concluded that, within the assumption stated above, carbons in each polymorph have equal average proximity to the crystallite surface. Normally this would mean that the two polymorphs were either intimately mixed or that the average lateral dimensions of the crystallites were the same. The differential response to hydrolysis of *Cladophora* cellulose eliminates the intimate mixing hypothesis, leaving only the latter conclusion.

A  $^{13}\text{C}$ - $^{13}\text{C}$  spin exchange experiment was conducted on both a highly crystalline algal cellulose (*Rhizoclonium*) and on hydrocellulose from cotton linters. This experiment probed the resonance profiles of  $^{13}\text{C}$  nuclei within, roughly, a 0.7-1.0 nm sphere surrounding a properly chosen, single resonance within a given multiplet. Spin populations of lines belonging to either the  $I_{\alpha}$  or  $I_{\beta}$  crystalline phase were selectively perturbed and the 'near-neighbor' spectra of those carbons involved in subsequent  $^{13}\text{C}$ - $^{13}\text{C}$  spin-exchange events were monitored. Qualitatively, the  $I_{\alpha}$  perturbations in the algal cellulose gave rise to  $I_{\alpha}$ -rich 'near-neighbor' spectra, compared with the original spectrum. Similarly,  $I_{\beta}$  perturbations yielded 'near-neighbor' spectra which were ' $I_{\beta}$ -rich'. In this way different environments within the algal celluloses were clearly identified, thereby, strongly supporting the thesis of crystalline polymorphy in the algal celluloses. Some details about the originally proposed spectra are called into question by these results; nevertheless, the existence of crystalline polymorphy in the algal celluloses seems abundantly clear. On the other hand, the spin exchange experiments performed on cotton hydrocellulose failed to detect the presence of any  $I_{\alpha}$  crystalline form, but the signal-to-noise levels were not adequate for eliminating the possibility of a minor amount of the  $I_{\alpha}$  form. These results differ considerably from the suggestions offered by Cael, et al (47), who, in an attempt to rationalize x-ray structural work and NMR spectra, identified two NMR component spectra based on a 2-chain or an

8-chain unit cell. They argued that algal celluloses consist of pure 8-chain unit cells, whereas higher plant celluloses, like ramie, are mixtures of 2-chain and 8-chain unit cells.

Finally, an attempt is made to isolate the true  $I_{\alpha}$  and  $I_{\beta}$  spectra, based on the original and hydrolyzed samples of Cladophora cellulose. Whereas the  $I_{\alpha}$  spectrum is nearly identical to that originally proposed (1-3), the  $I_{\beta}$  spectrum is ambiguous and two possible spectra are proposed.

In contrast to the polymorphic algal and bacterial celluloses, which contain large fractions of the  $I_{\alpha}$  and  $I_{\beta}$  polymorphs, the higher plant celluloses are dominated by the  $I_{\beta}$  crystalline form with only a minor, if any,  $I_{\alpha}$  component. The shape of the C4 resonance in the higher plant celluloses is evidence, especially if no  $I_{\alpha}$  component exists, of a unit cell containing more than four anhydroglucose residues. In view of these findings, the crystal structures of native cellulose based on Valonia cellulose should be reexamined, and assumptions about symmetry in the unit cell of the higher plant celluloses should be reconsidered.

#### Acknowledgment

We wish to express our profound thanks to Dr. J.-F. Revol of the Pulp and Paper Research Institute of Canada for his interest, discussions, and his willingness to characterize the lateral dimensions of crystallites in certain of the algal cellulose preparations.

#### Literature Cited

1. VanderHart, D. L.; Atalla, R. H. Preprints of the International Dissolving and Specialty Pulps Conference: Boston, 1983, p. 207.
2. Atalla, R. H.; VanderHart, D. L. Science 1984, 223, 283.
3. VanderHart, D. L.; Atalla, R. H. Macromolecules 1984, 17, 1465.
4. Frey-Wyssling, A.; Muhlethaler, K. Makromol. Chem. 1963, 62, 25.
5. Manley, R. St.J. J. Polym. Sci. Part A-2 1971, 9, 1025.
6. Blackwell, J.; Kolpak, F. J. Macromolecules 1975, 8, 322.
7. Lazaro, R.; Chiverina, J. Cell. Chem. Technol. 1973, 7, 269.
8. Roche, E.; Chanzy, H. Int. J. Biol. Macromol. 1981, 3, 201.
9. Goto, T; Harada, H.; Saiki, H. Mokuzai Gakkaishi 1973, 19, 463.
10. VanderHart, D. L. Deductions about the Morphology of Wet and Wet Beaten Celluloses from Solid State  $^{13}\text{C}$  NMR, NBSIR 82-2534.
11. Dudley, R. L.; Fyfe, C. A.; Stephenson, P. J.; Deslandes, Y.; Hamer, G. R.; Marchessault, R. H. J. Am. Chem. Soc. 1983, 105, 2469.
12. Wellard, H. J. J. Polym. Sci. 1954, 13, 471.
13. Honjo, G.; Watanabe, M. Nature 1958, 181, 326.
14. Meyer, K. H.; Misch, L. Helv. Chim. Acta. 1937, 20, 232.



15. Ellis, K. C.; Warwicker, J. O. J. Polym. Sci. 1962, 56, 339.
16. Gardener, K. H.; Blackwell, J. Biopolymers 1975, 14, 1581.
17. Sarko, A.; Muggli, R. Macromolecules 1974, 7, 486.
18. French, A. D. Carbohydr. Res. 1978, 61, 67.
19. Marrinan, H. J.; Mann, J. J. J. Polym. Sci. 1956, 21, 301.
20. Revol., J.-F.; Goring, D. A. I. Polymer 1983, 24, 1547.
21. Revol., J.-F., personal communication.
22. VanderHart, D. L.; Earl, W. L.; Garroway, A. N. J. Magn. Res. 1981, 44, 361.
23. Earl, W. L.; VanderHart, D. L. Macromolecules 1981, 14, 570.
24. Hartmann, S. R.; Hahn, E. L. Phys. Rev. 1962, 128, 2042.
25. Pines, A.; Gibby, M. G.; Waugh, J. S. J. Chem. Phys. 1973, 59, 569.
26. Andrew, E. R.; Bradbury, A.; Eades, R. G. Nature (London) 1958, 182, 1659.
27. Lowe, I. J. Phys. Rev. Lett. 1959, 2, 285.
28. Bodenhausen, G.; Freeman, R.; Morris, G. A. J. Magn. Res. 1976, 23, 171.
29. Morris, G. A.; Freeman, R. J. Magn. Res. 1978, 29, 433.
30. Caravatti, P.; Bodenhausen, G.; Ernst, R. R. J. Magn. Res. 1983, 55, 88.
31. Torchia, D. A. J. Magn. Res. 1978, 30, 613.
32. VanderHart, D. L. J. Magn. Res., in press.
33. Browning, B. L. Methods of Wood Chemistry; Interscience Publishers: New York, 1967.
34. Atalla, R. H.; Gast, J. C.; Sindorf, D. W.; Bartuska, V. J.; Maciel, G. E. J. Am. Chem. Soc. 1980, 102, 3249.
35. Earl, W. L.; VanderHart, D. L. J. Am. Chem. Soc. 1980, 102, 3251.
36. Horii, F.; Hirai, A.; Kitamaru, R. Polym. Bull. 1982, 8, 1963.
37. Haigler, C. H.; Brown, R. M., Jr.; Benjamin, M. Science, 1980, 210, 903.
38. Nelson, M. L.; Tripp, V. W. J. Polym. Sci. 1953, 10, 577.
39. Abragam, A. Principles of Nuclear Magnetism; Oxford University Press: London, 1961.
40. Douglass, D. C.; Jones, G. P. J. Chem. Phys. 1966, 45, 956.
41. Horii, F.; Hirai, A.; Kitamaru, R. J. Carbohydr. Chem. 1984, 3, 641.
42. Packer, K. J.; Pope, J. M.; Young, R. R.; Cudby, M. E. A., J. Polym. Sci. Polym. Phys. Ed. 1984, 22, 589.
43. Havens, J. R.; VanderHart, D. L. Macromolecules 1985, 18, 1663.
44. Vega, A. J.; Vaughan, R. W. J. Chem. Phys. 1978, 68, 1958.
45. Teeäär, R.; Lippmaa, E. Polym. Bull. 1984, 12, 315.
46. VanderHart, D. L.; Garroway, A. N. J. Chem. Phys. 1979, 71, 2773.
47. Cael, J. J.; Kwoh, D. L. W.; Bhattacharjee, S. S.; Patt, S. L. Macromolecules 1985, 18, 821.
48. Atalla, R. H. Adv. Chem. Ser. 1979, No. 181, p. 55.

49. Atalla, R. H. Proceedings at the International Symposium on Wood and Pulping Chemistry, Stockholm, June 1981.
50. Atalla, R. H. Proceedings at the 9th Cellulose Conference, May 1982.

## Figure Captions

Figure 1. Originally proposed  $^{13}\text{C}$  CP-MAS NMR spectra for the crystalline allomorphs,  $I_{\alpha}$  and  $I_{\beta}$ ; included are the assignments of the various carbon resonances. These spectra were generated by linear combination and were based on spectra of Acetobacter xylinum cellulose and a low-DP regenerated cellulose I. Gaps in the spectra appear where the first spinning sideband of polyethylene, the chemical shift standard, occurred.

Figure 2. 50 MHz CP-MAS  $^{13}\text{C}$  spectra of cotton linters (A: dry; B: wet) and Valonia ventricosa (C). All spectra are normalized to the same total intensity.

Figure 3. CP-MAS  $^{13}\text{C}$  spectra of various higher plant celluloses in comparison with the algal cellulose spectrum of Cladophora (lower).

Figure 4. 50 MHz  $^{13}\text{C}$  CP-MAS spectra of bacterial and algal celluloses: A and B: two preparations of Acetobacter xylinum; C: Cladophora glomerata, beaten at 1% solids consistency, D: Cladophora glomerata, E: Valonia macrophysa, F: Rhizoclonium hieroglyphicum, and G: Valonia ventricosa.

Figure 5. Effect of acid hydrolysis on the  $^{13}\text{C}$  CP-MAS spectrum of cotton linters. A: Original material, B: subjected to 2.5N HCl for 30 min, and C: a renormalized linear combination spectrum  $[4x(A-.72B)]$ . Spectrum A and B are normalized to the same total intensity.

Figure 6.  $^{13}\text{C}$  CP-MAS spectra, normalized to the same intensity, of various preparations of Cladophora cellulose: A: original, B: after beating in a Waring Blender at 1% solids consistency, C: after beating in a Waring Blender at 3% solids consistency, D: after acid hydrolysis (4N HCl, 100C, 44h) of the beaten (1%) sample (22% mass recovery), E: after acid hydrolysis, as above, of an unbeaten second strain of Cladophora (12% mass recovery).

Figure 7. CP-MAS spectra of cotton hydrocellulose following the two indicated periods of proton spin locking; the CP time was 0.5 ms. Spectrum B is renormalized to match the intensity in A for the crystalline C4 resonance; true total intensities are also given. The difference spectrum, (A-B), shows the profile of resonances with shorter  $T_{1\rho}$  values. The lower lineshape involving the spectrum (not shown) with a 15 ms proton spin lock, indicates that there are no further lineshape changes after 15 ms of spin locking.

Figure 8. CP-MAS spectra of the highly crystalline algal cellulose, Rhizoclonium hieroglyphicum as a function of proton spin locking time.

Figure 9. CP-MAS spectra of hydrocellulose from cotton linters as a function of the indicated delay time in a  $T_1^C$  experiment [Ref. 31].

Figure 10. CP-MAS spectra of Cladophora cellulose as a function of the indicated delay times in a  $T_1^C$  experiment. Total intensities are also given.

Figure 11. Spectral method for isolating the 'near-neighbor' spectrum of an  $I_\alpha$  line in Rhizoclonium cellulose. The number of scans is 1200 for spectra A and B, 600 for C and D. See text for other details.

Figure 12. CP-MAS spectra of Rhizoclonium cellulose associated with three different 'near-neighbor' experiments.

Figure 13. CP-MAS spectra of hydrocellulose from cotton linters associated with two 'near-neighbor' spectra obtained after 50s of spin exchange. The format is the same as in Figure 12.

Figure 14. Candidates for  $I_\alpha$  and  $I_\beta$  CP-MAS spectra based on the spectra of Cladophora (A) and acid hydrolyzed Cladophora (B) celluloses. Proportions of mixing for spectra C-E are indicated in the figures for the linear combination spectra, which are further renormalized to give the same total intensities as in A and B. Spectrum C is the  $I_\alpha$  spectrum; spectrum D and E are two candidates for the  $I_\beta$  spectrum.

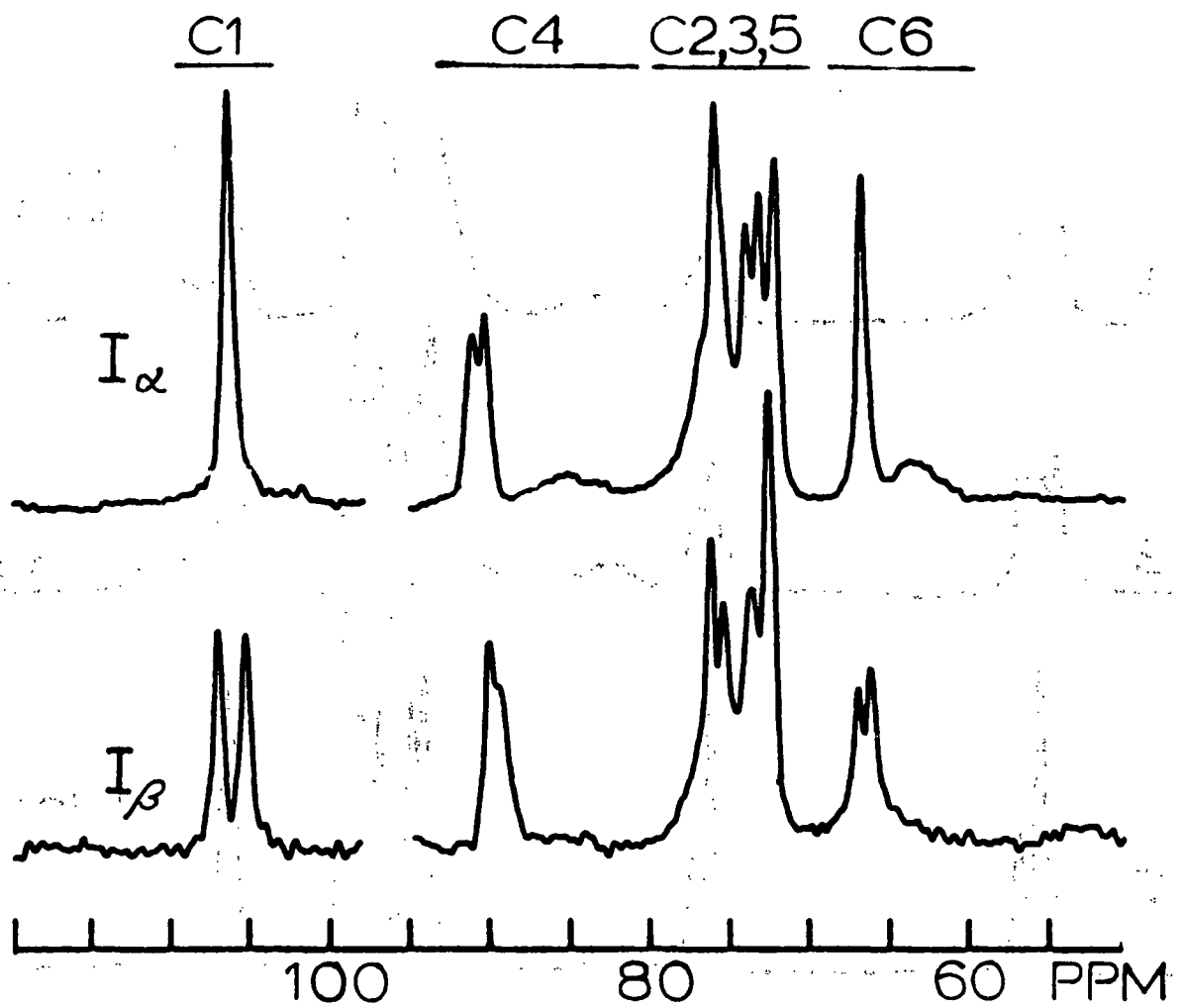


FIGURE 1

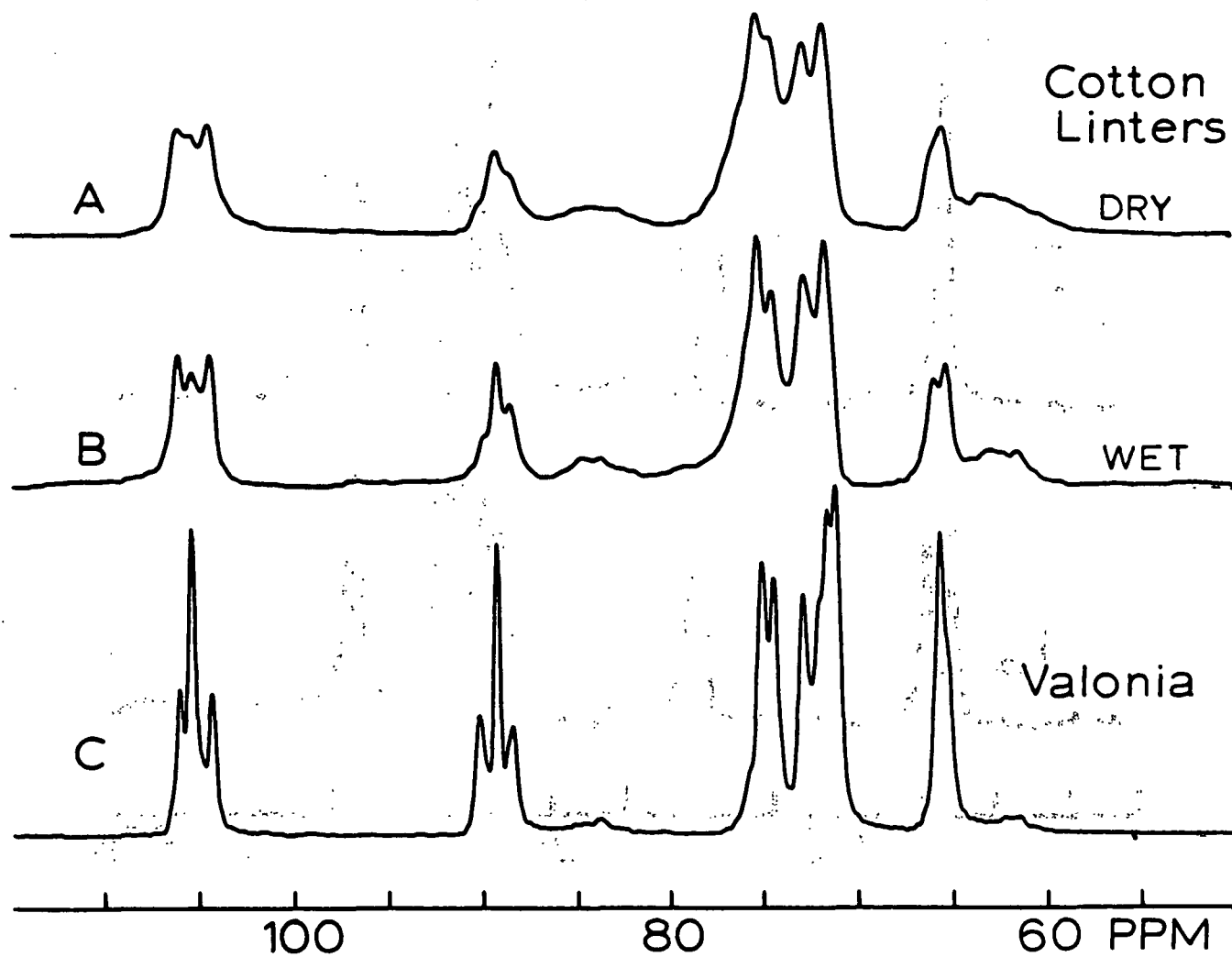


FIGURE 2

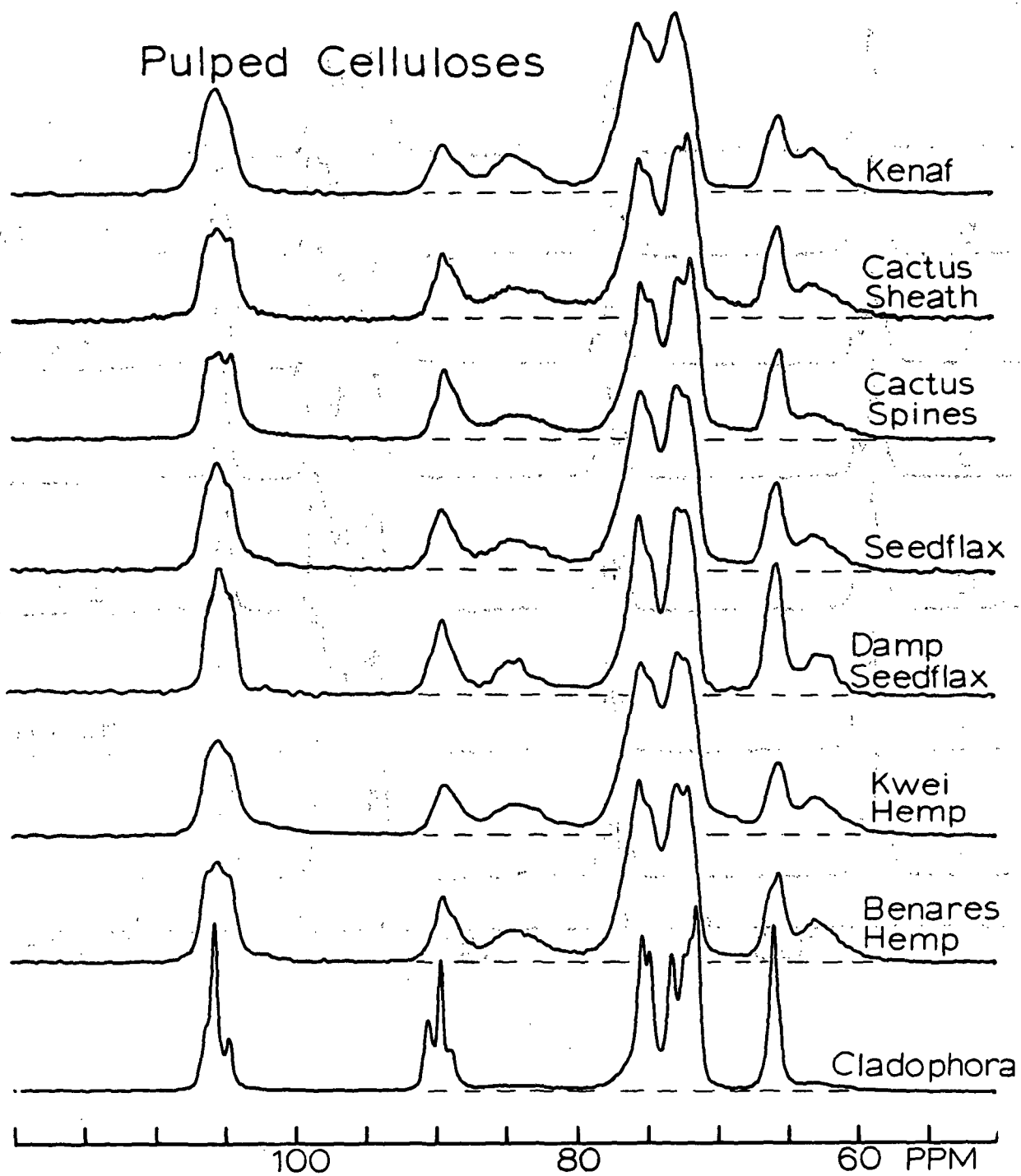


FIGURE 3

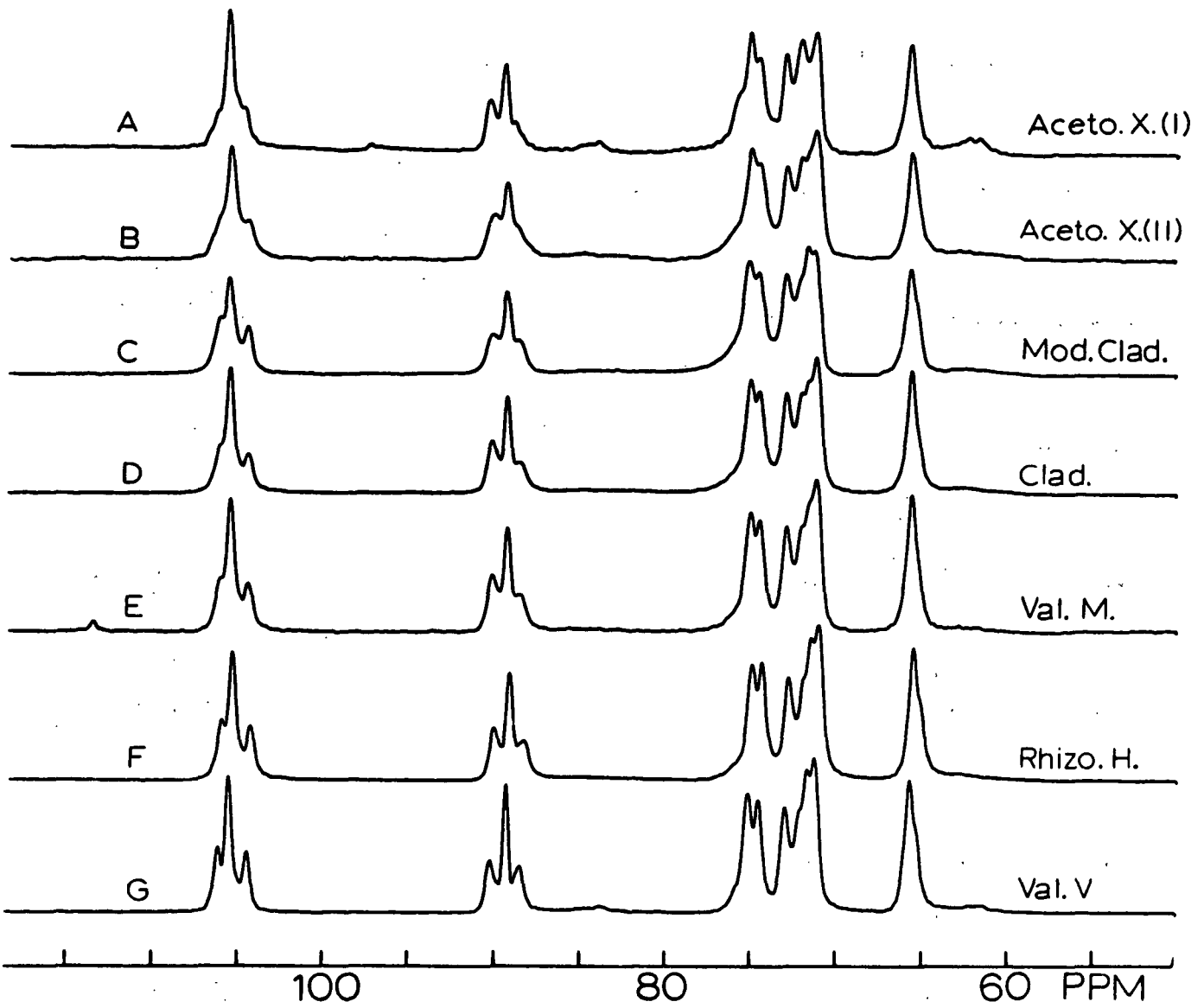


FIGURE 4



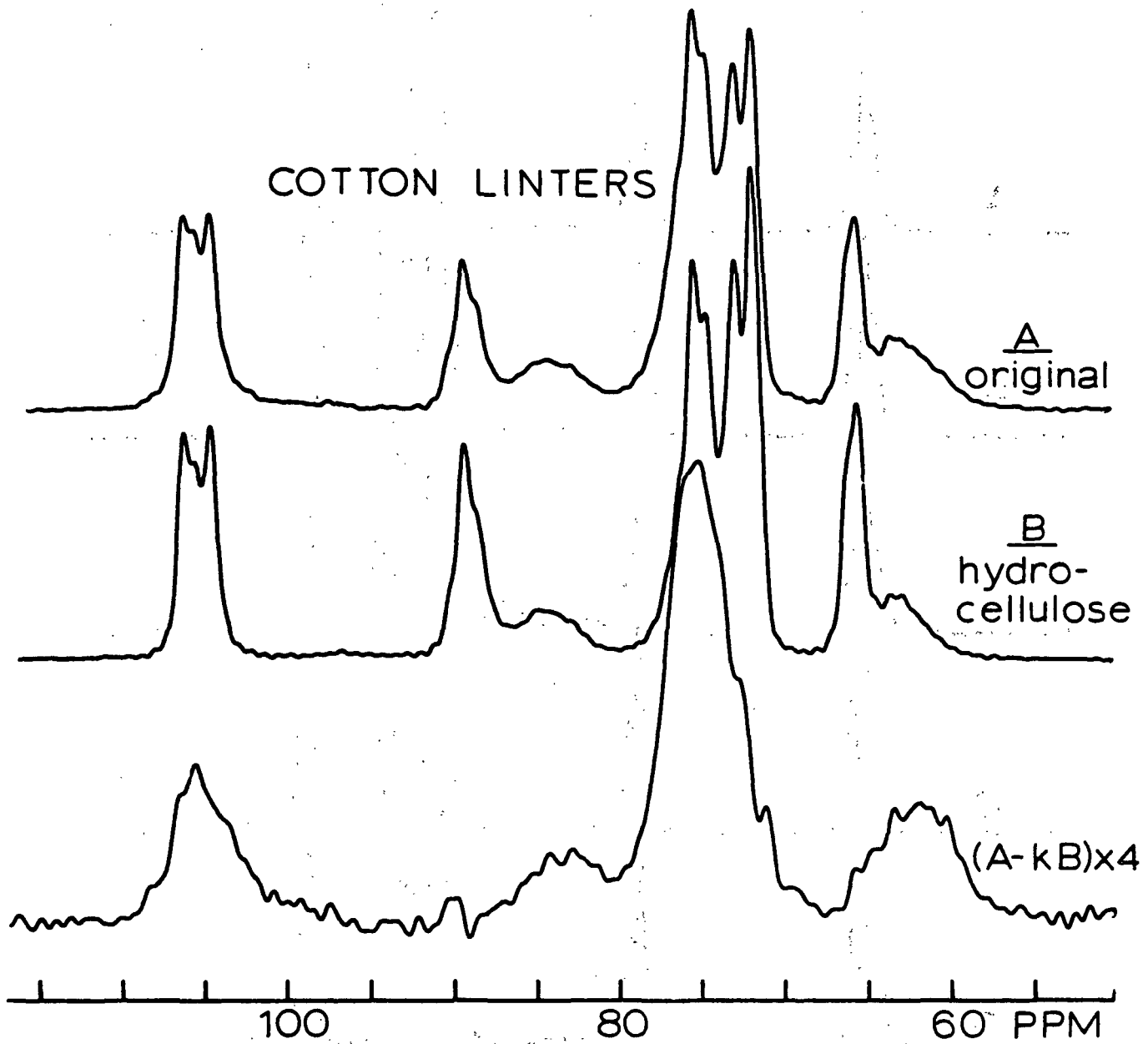


FIGURE 5

Cladophora

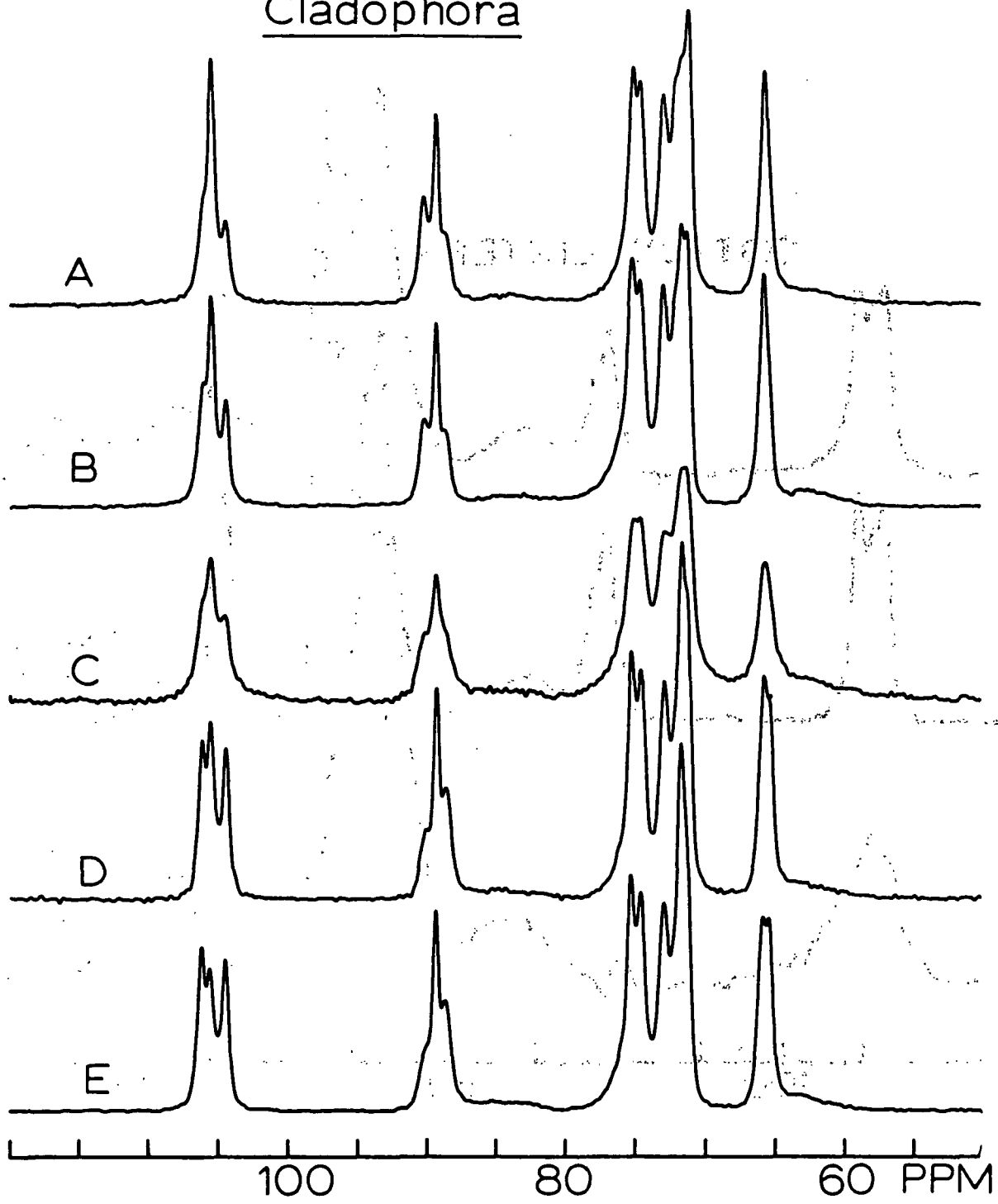


FIGURE 6

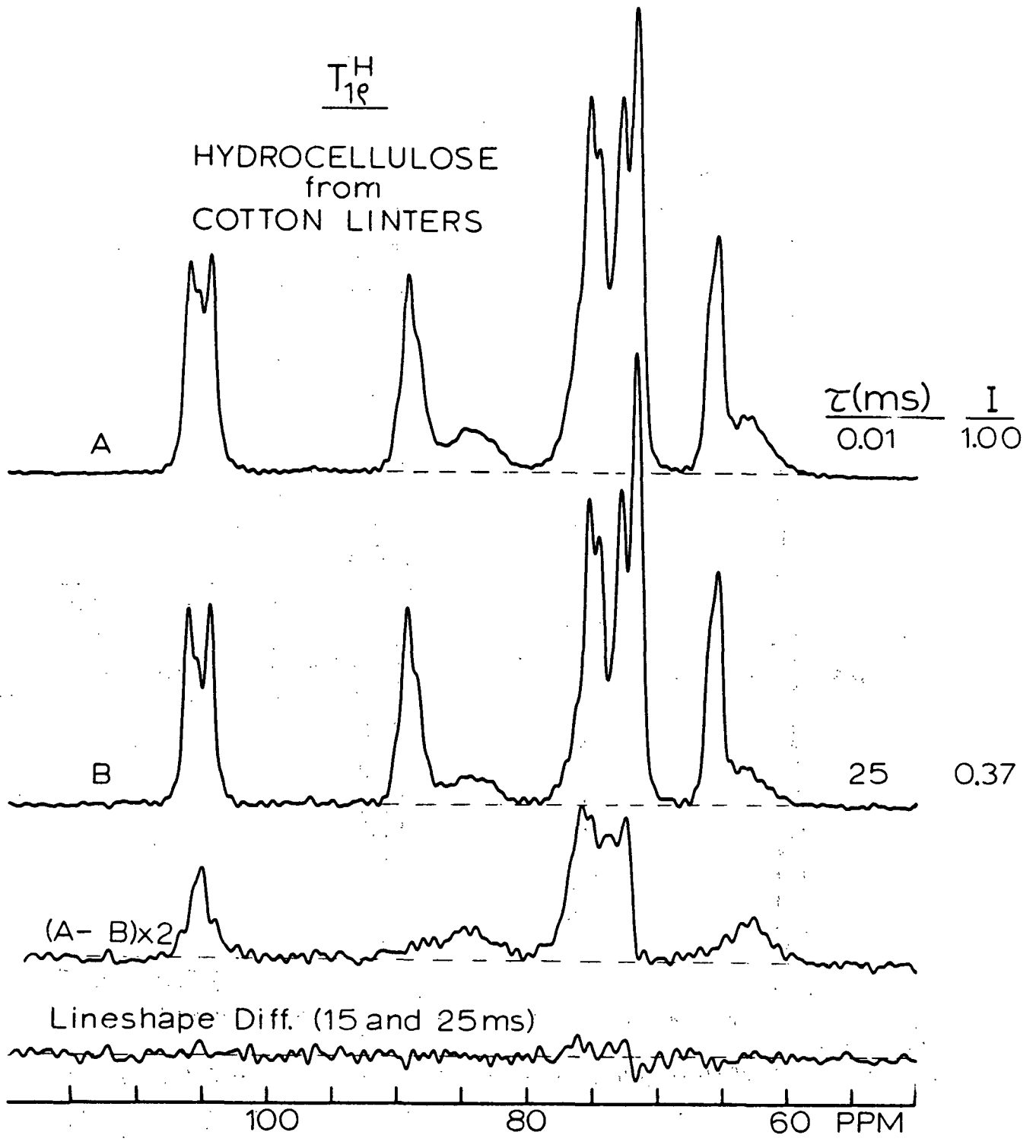


FIGURE 7

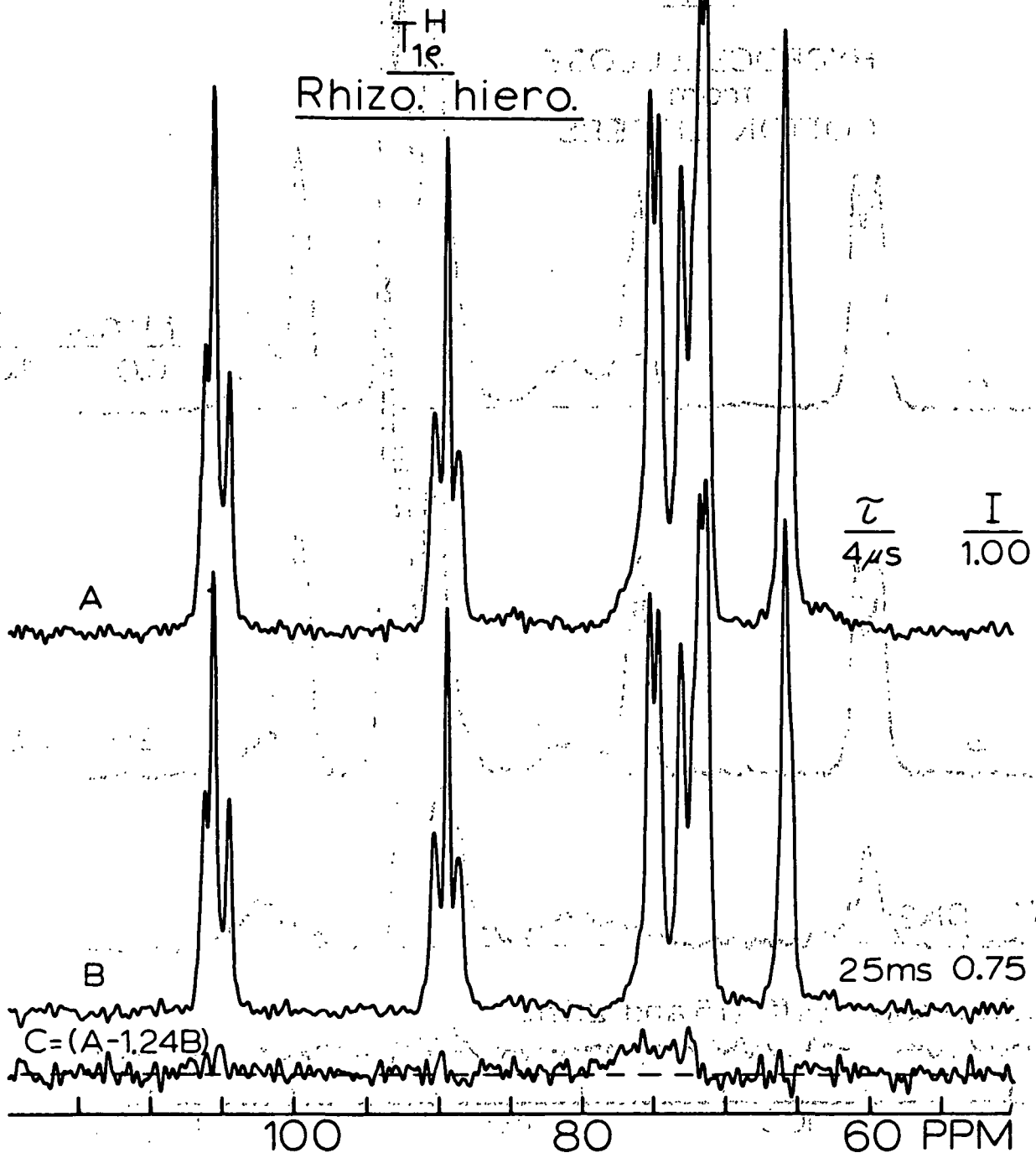


FIGURE 8

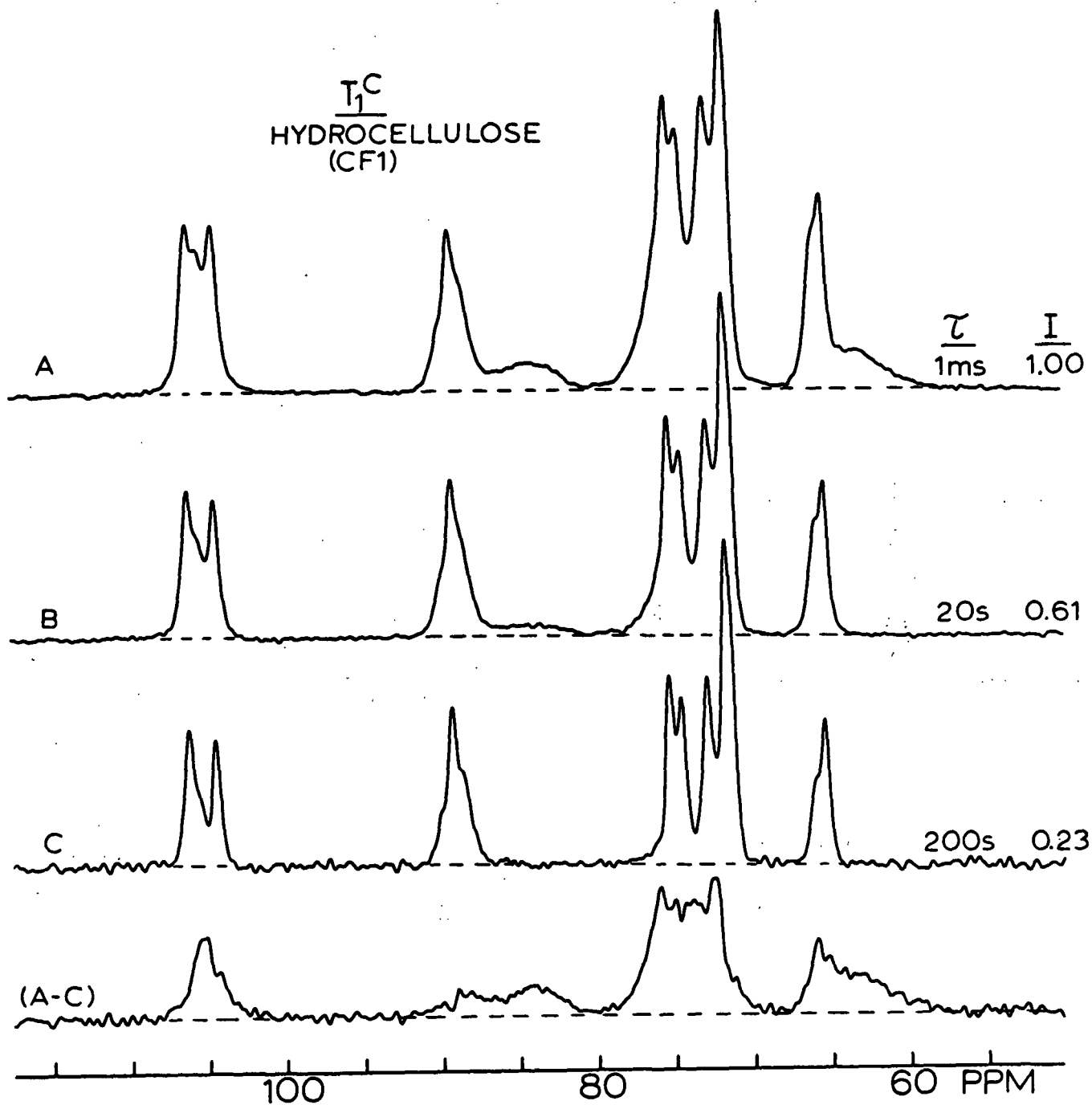


FIGURE 9

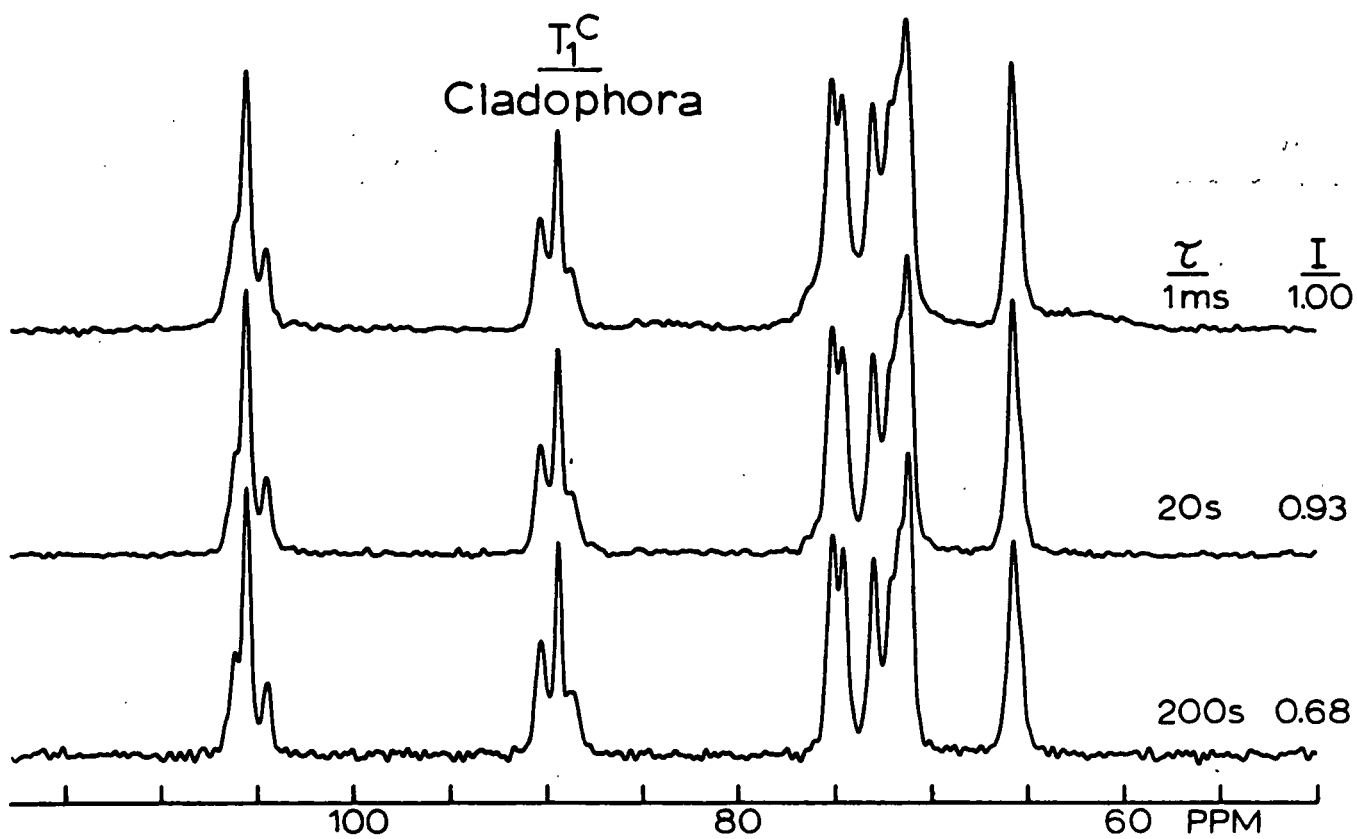


FIGURE 10

RHIZO. HIERO.

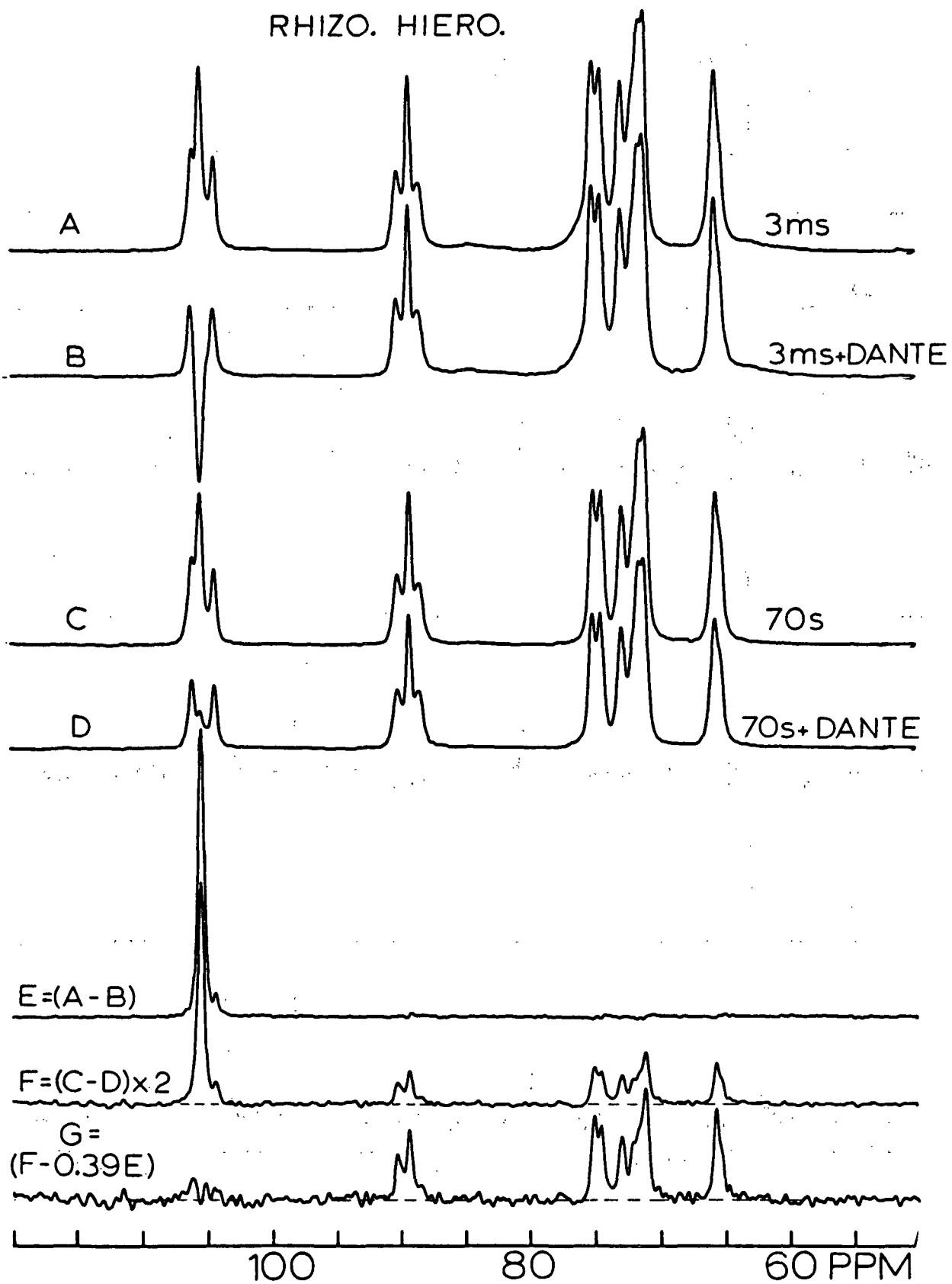


FIGURE 11

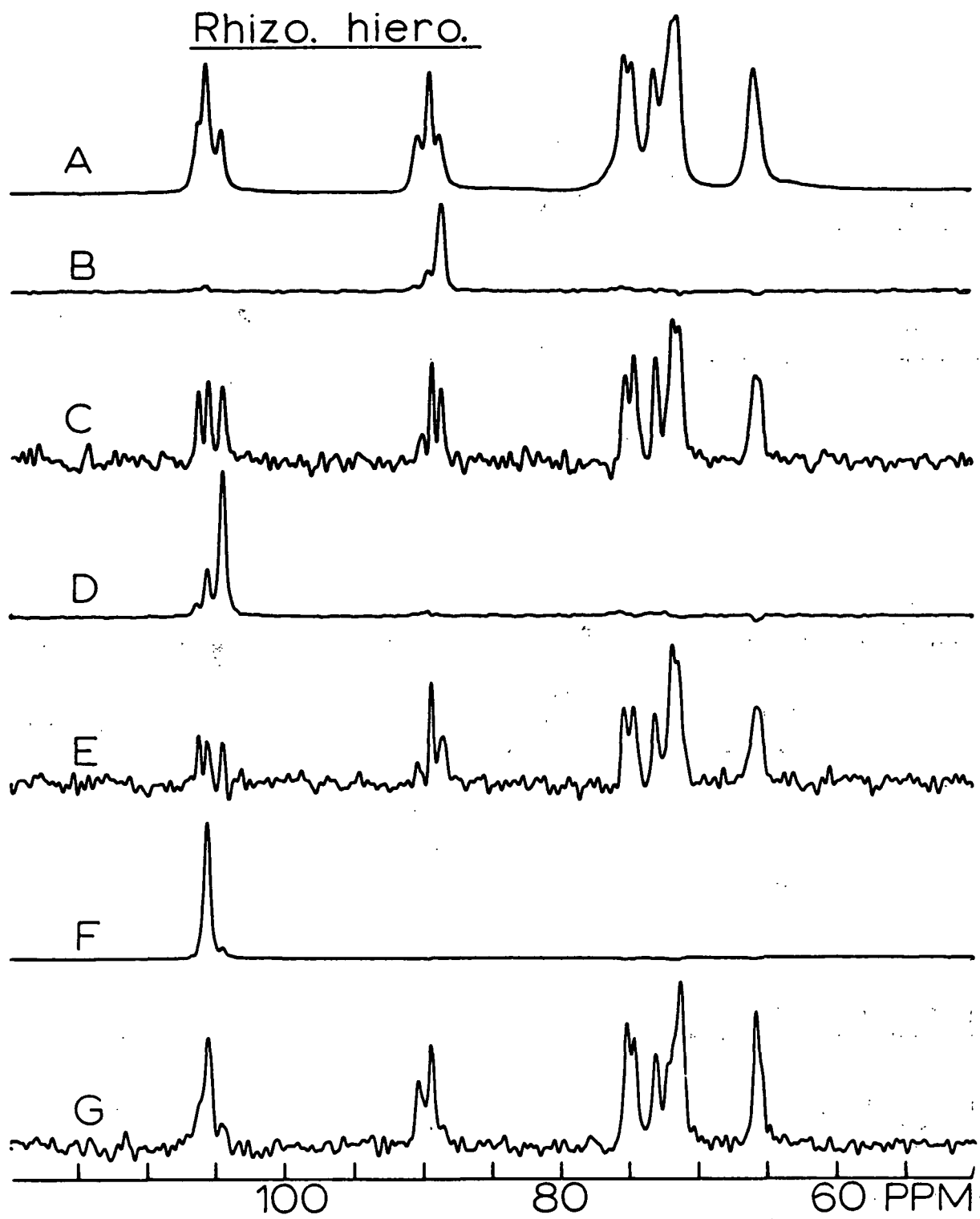


FIGURE 12



Hydrocellulose

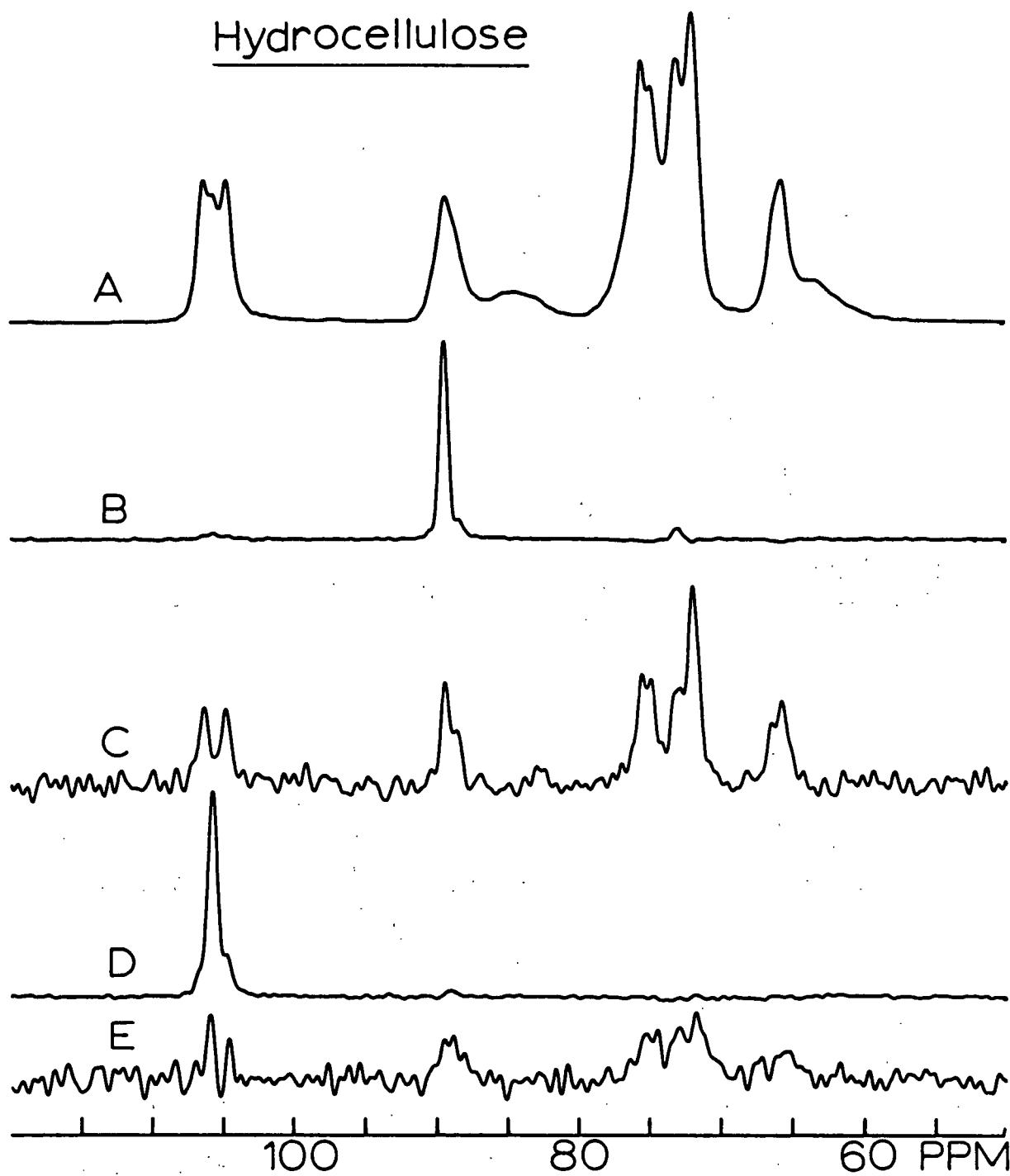


FIGURE 13

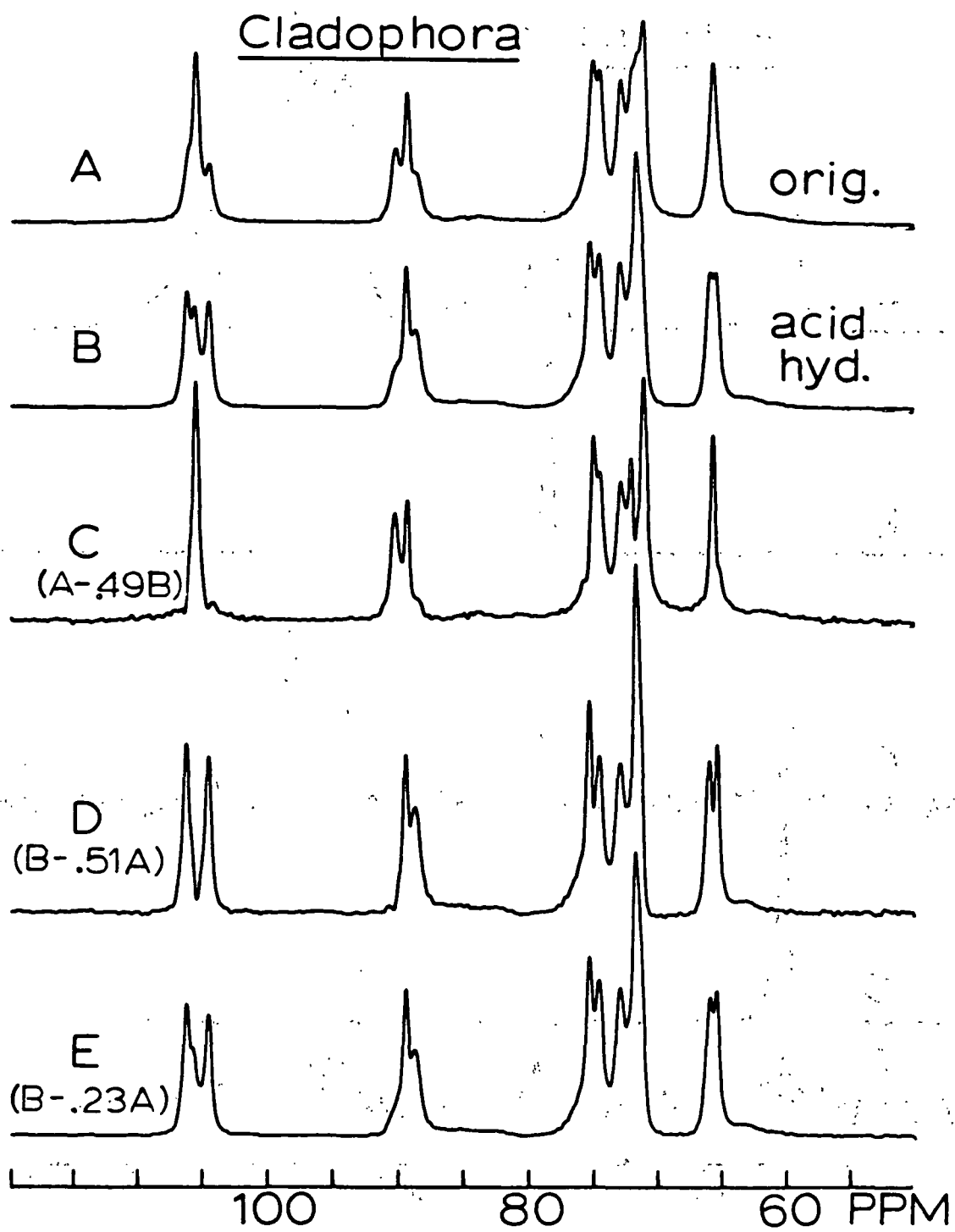


FIGURE 14